Bioorganic & Medicinal Chemistry xxx (2016) xxx–xxx

Contents lists available at ScienceDirect

Bioorganic & Medicinal Chemistry

journal homepage: www.elsevier.com/locate/bmc

Synthesis and structure activity relationships of glycine amide derivatives as novel Vascular Adhesion Protein-1 inhibitors

Susumu Yamaki *, Daisuke Suzuki, Jiro Fujiyasu, Masahiro Neya †, Akira Nagashima, Mitsuhiro Kondo, Takafumi Akabane, Keitaro Kadono, Ayako Moritomo, Kosei Yoshihara ‡

Drug Discovery Research, Astellas Pharma Inc., 21 Miyukigaoka, Tsukuba, Ibaraki 305-8585, Japan

ARTICLE INFO

Article history:
Received 20 September 2016
Revised 18 October 2016
Accepted 19 October 2016
Available online xxxx

Keywords:
Vascular Adhesion Protein-1
Diabetic microvascular complication
Glycine amide
PAMPA

ABSTRACT

Vascular Adhesion Protein-1 (VAP-1) is a promising therapeutic target for the treatment of several inflammatory-related diseases including diabetic microvascular complication. We identified glycine amide derivative **3** as a novel structure with moderate VAP-1 inhibitory activity. Structure-activity relationship studies of glycine amide derivatives revealed that the tertiary amide moiety is important for stability in rat blood and that the position of substituents on the left phenyl ring plays an important role in VAP-1 inhibitory activity. We also found that low TPSA values and weak basicity are both important for high PAMPA values for glycine amide derivatives. These findings led to the identification of a series of orally active compounds with enhanced VAP-1 inhibitory activity. Of these compounds, **4g** exhibited the most potent ex vivo efficacy, with plasma VAP-1 inhibitory activity of 60% after oral administration at 1 mg/kg.

1. Introduction

Vascular Adhesion Protein-1 (VAP-1) is a member of the family of copper-containing amine oxidases/semicarbazide-sensitive amine oxidase (AOC/SSAO), found in humans as a membrane-bound form and a soluble form. The membrane-bound form of VAP-1 is mainly expressed in endothelial cells, smooth muscle cells, and adipocytes, whereas the soluble VAP-1 is released into plasma mainly from vascular endothelial cells.[1]

VAP-1 is reported to have two functions. As an adhesion molecule, VAP-1 is involved in leukocyte rolling, adhesion and transmigration, which are central steps in leukocyte extravasation to sites of inflammation.[2] Another function of VAP-1 is to act as an amine oxidase. It possesses topaquinone (TPQ) in the active site as a cofactor, and catalyzes the conversion of primary amines (e.g., methylamine and aminoacetone) into the corresponding aldehydes (e.g., formaldehyde and methylglyoxal), while releasing ammonia and hydrogen peroxide (Eq. (1)).[3]

$$RCH_2NH_2 + O_2 + H_2O \rightarrow RCHO + H_2O_2 + NH_3 \quad (1)$$

Increased plasma and/or membrane associated VAP-1 activities have been found in patients with diabetic mellitus, and even more so in patients with diabetic microvascular complication such as diabetic retinopathy and diabetic nephropathy.[4] Elevated expression of VAP-1 results in increased production of enzymatic products of VAP-1 like aldehyde and hydrogen peroxide. These products have been reported to participate in the development of diabetic microvascular complication, for example, by inducing oxidative stress.[5] Further, plasma and/or membrane bound VAP-1 is also increased, and is suggested to be involved in diseases such as rheumatoid arthritis,[6] atherosclerosis,[7] chronic heart failure[8] and Alzheimer's disease.[9] All of which are associated with inflammation. These facts suggest that VAP-1 is a promising therapeutic target for the treatment of several inflammatory-related diseases, including diabetic microvascular complication.

Several approaches to inhibit VAP-1 have been reported, including small interfering RNAs, function blocking antibodies, and small molecule inhibitors.[1,10] Among these, Bioite Therapeutics is conducting clinical trials with their anti-VAP-1 antibody (BTT-1023) for the treatment of autoimmune inflammatory and fibrotic diseases.[11] As for small molecule inhibitors, PXS-4728A (**1**) (IC_{50} = 5 nM[12]) has recently advanced to clinical trials for treatment of non-alcoholic steatohepatitis (NASH) (Fig. 1).[12]

We have previously reported a novel VAP-1 inhibitor, compound **2**, which showed potent VAP-1 inhibitory activity with an IC_{50} value of 0.019 μM (Fig. 1).[13c] Oral administration of this

* Corresponding author. Tel.: +81 29 863 6550; fax: +81 29 852 5387.
E-mail address: susumu.yamaki@astellas.com (S. Yamaki).
† Present address: KNC Laboratories Co., Ltd, 1-1-1 Murotani, Nishiku, Kobe, Hyogo 651-2241, Japan.
‡ Present address: Haupt Pharma Toride Co., Ltd, 5662 Omonmai, Toride, Ibaraki 302-0001, Japan.

http://dx.doi.org/10.1016/j.bmc.2016.10.025
0968-0896/

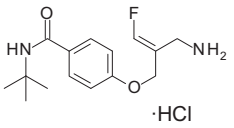

PXS-4728A (**1**)

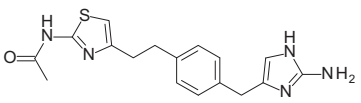

2

Figure 1. Structures of PXS-4728A (**1**) and **2**.

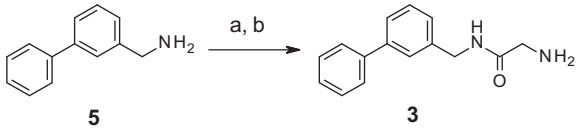

Scheme 1. Reagents and conditions: (a) *N*-(*tert*-butoxycarbonyl)glycine, WSCD·HCl, HOBt, DMF; (b) 4 M HCl (EtOAc solution).

compound at 10 mg/kg showed an inhibitory effect on ocular permeability in streptozotocin (STZ)-induced diabetic rats. These results suggested that VAP-1 would be a promising therapeutic target for the treatment of diabetic macular edema. However, this compound was not suitable for further clinical development due to its insufficient pharmacokinetic properties in rats ($F = 0.7\%$). These facts prompted us to identify novel VAP-1 inhibitors.

To find a novel class of orally active VAP-1 inhibitors, we screened our in-house compound library for VAP-1 enzymatic inhibitory activity and identified compound **3** as a moderate VAP-1 inhibitor with an IC_{50} value of 0.18 μM (Table 1). Although this compound possesses a novel scaffold with moderate VAP-1 inhibitory activity, **3** showed poor ex vivo efficacy (17% inhibition in rat plasma VAP-1 activity after oral administration at 100 mg/kg). We therefore conducted structural optimization of **3** in order to improve its ex vivo efficacy. In this manuscript, we describe the synthesis and structure-activity relationships of glycine amide derivatives as novel VAP-1 inhibitors.

2. Chemistry

The synthesis of glycine amide derivatives is outlined in Schemes 1–6. Condensation of benzylamine **5** with *N*-(*tert*-butoxycarbonyl)glycine followed by deprotection of *tert*-butoxycarbonyl (Boc) group gave **3** (Scheme 1). Scheme 2 shows the synthesis of **4a**–**4h**. Condensation of benzylamine **6** with *N*-Boc-glycine gave **7**. Suzuki coupling of **7** with various boronic acids or esters followed by removal of Boc group afforded **4a**–**4h**.

Compounds **10**, **11a**–**11d**, **12a**–**12b**, and **13** were prepared by the synthetic scheme depicted in Scheme 3. Suzuki coupling between **7** and corresponding boronic acids or esters gave biphenyl analogs **8a**–**8c**. Hydrolysis and removal of Boc group of **8a** by treatment with 6 M HCl at 100 °C yielded **10**. Hydrolysis of **8a** by NaOH gave carboxylic acid **9**, which was then converted into amide derivatives **11a**–**11d** by condensation with a variety of amines and subsequent deprotection of Boc group. Treatment of aniline **8b** with carbamoyl chlorides followed by removal of Boc group yielded **12a**–**12b** respectively. Reductive amination of aldehyde **8c** with diethylamine followed by removal of Boc group gave benzylamine analog **13**.

Scheme 4 shows the synthesis of compounds **17**–**19**. Suzuki coupling between aryl bromide **14** with **15** followed by deprotection of Boc group gave benzylamine **16**. Benzylamine **16** was then converted into **17**–**19** by condensation with the corresponding amino acids and subsequent removal of Boc group.

The synthesis of **27**–**30** is shown in Scheme 5. Condensation of benzylamine **6**, **20** or isoindoline **22** with appropriate amino acids afforded **23**, **24** and **26**. Substitution of benzylbromide **21** with *tert*-butyl [2-(methylamino)ethyl]carbamate gave **25**. Suzuki coupling of the resulting **23**–**26** with **15** followed by deprotection of Boc group gave **27**–**30**.

Benzamide derivative **33** was synthesized as shown in Scheme 6. Suzuki coupling between aryl bromide **31** and **15** followed by hydrolysis using NaOH gave carboxylic acid **32**. Condensation of **32** with *tert*-butyl [2-(methylamino)ethyl]carbamate followed by removal of Boc group gave compound **33**.

3. Results and discussion

The inhibitory activities of the synthesized compounds against human and rat VAP-1 were measured by a radiochemical-enzyme assay using ^{14}C-benzylamine as an artificial substrate. Plasma VAP-1 activities in normal rats after oral administration of test compounds were evaluated by using the same radiochemical-enzyme assay.

We identified glycine amide derivative **3** as a novel structure from our in-house compound library. This compound showed moderate VAP-1 inhibitory activity with an IC_{50} value of 0.18 μM. However, it showed poor ex vivo efficacy (17% inhibition in rat plasma VAP-1 activity after oral administration at 100 mg/kg) in spite of the fact that there were no particular problems with solubility, membrane permeability, or metabolic stability in liver microsomes (data not shown). Since an amide bond would be sometimes vulnerable to hydrolysis, we suspected the stability of this compound in vivo and examined its stability in rat blood. As shown in Figure 2, it was found that concentration of **3** was decreased to 33% after incubation with rat blood for 1 h. Therefore, we considered that instability of **3** in rat blood is one of the reasons for low ex vivo activity. Because we needed to confirm the activity of compounds in rodent, such as rat, before advancing to clinical trial, we considered it important to improve stability in rat blood to obtain a compound showing potent ex vivo efficacy. Testa

Table 1
In vitro and pharmacodynamic profile of **3**

Compound	Structure	Human VAP-1 IC_{50} (μM)[a]	Rat ex vivo[b]	
			Dose (mg/kg, po)	Inhibition ratio (at 1 h) (%)
3[c]	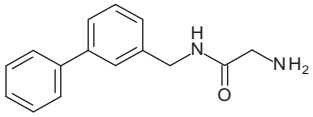	0.18	100	17

[a] IC_{50} value is shown as the mean of independent experiments ($n = 2$).
[b] Inhibitory effect on plasma VAP-1 activity in rats ($n = 5$) at 1 h after oral administration of compound **3**.
[c] Hydrochloride salt.

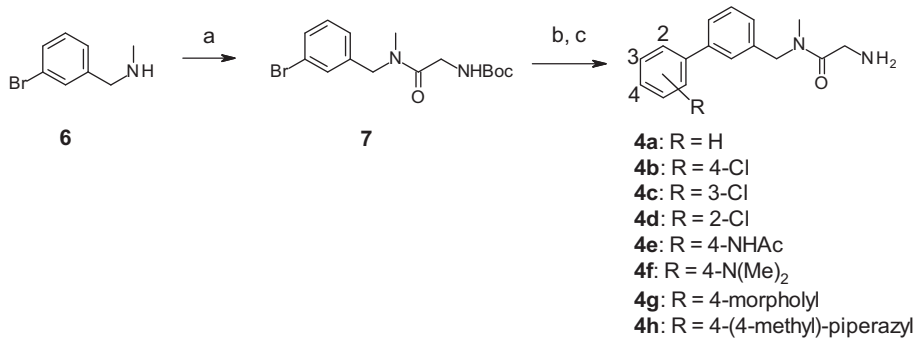

Scheme 2. Reagents and conditions: (a) *N*-(*tert*-butoxycarbonyl)glycine, WSCD·HCl, HOBt, CH_2Cl_2; (b) Ar-B(OH)$_2$ or Ar-B(Pin), Pd(PPh$_3$)$_4$, Na_2CO_3, solvents, 80 °C; (c) 4 M HCl (EtOAc solution), EtOAc.

et al. reported that a tertiary amide would be more stable than the secondary amide against hydrolysis in the case of amides with bulky substituents on nitrogen.[14] Thus, we investigated the effect of conversion from secondary amide into tertiary amide on the stability in rat blood. As expected, tertiary amide derivative **4a** was found to be more stable in rat blood compared to **3**, with no apparent decrease in **4a** was observed even after incubation with rat blood for 6 h (Fig. 2). However, in vitro potency of **4a** to both human and rat VAP-1 enzyme were decreased more than 4-fold (human IC_{50} = 0.80 μM, rat IC_{50} = 0.12 μM) compared to that of **3** as shown in Table 2. In spite of its decreased in vitro potency, **4a** exhibited more potent ex vivo efficacy than **3** (**3**: 17% inhibition at 100 mg/kg, **4a**: 69% inhibition at 60 mg/kg). We speculated that **4a** has a higher plasma concentration than **3** because of its improved stability in rat blood. These results suggested that conversion to the tertiary amide from the secondary amide is important for stability in rat blood and results in potentiation of ex vivo efficacy. We expected that an improvement in the VAP-1 inhibitory activity of **4a** while maintaining stability in rat blood would lead to a compound with more potent ex vivo activity. Thus,

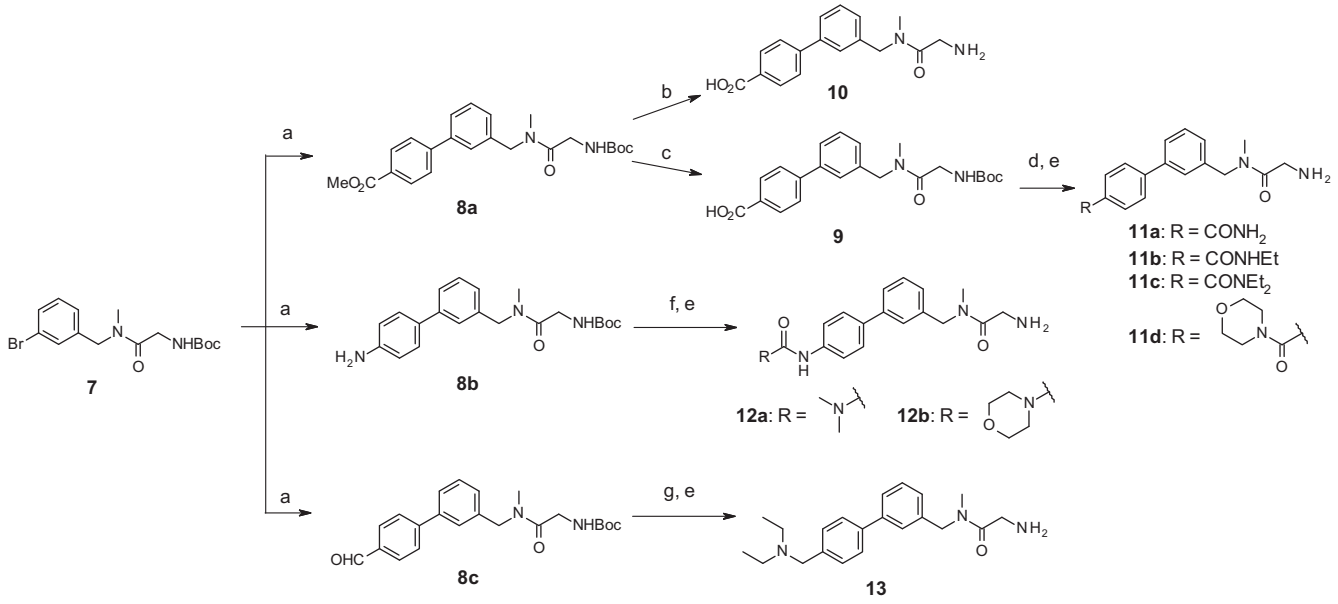

Scheme 3. Reagents and conditions: (a) Ar-B(OH)$_2$ or Ar-B(Pin), Pd(PPh$_3$)$_4$, Na_2CO_3, DME/EtOH/H_2O, 80 °C; (b) 6 M HCl aq, 100 °C; (c) 1 M NaOH aq, MeOH; (d) amine, WSCD·HCl or WSCD, HOBt, with or without Et_3N, DMF; (e) 4 M HCl (EtOAc solution), solvents; (f) carbamoyl chloride, base, CH_2Cl_2; (g) diethylamine, NaBH(OAc)$_3$, AcOH, DCE.

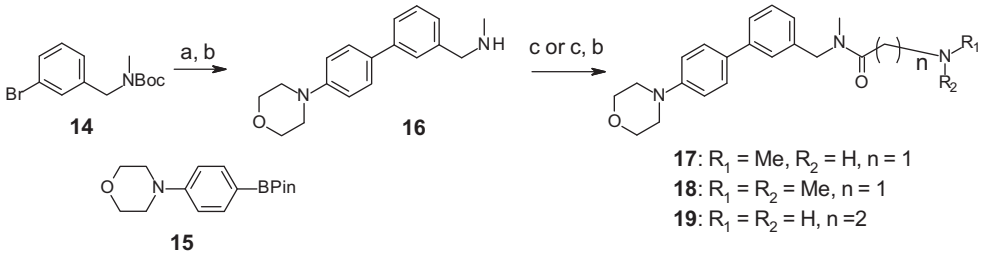

Scheme 4. Reagents and conditions: (a) **15**, Pd(PPh$_3$)$_4$, Na_2CO_3, DME/H_2O, 90 °C; (b) 4 M HCl (EtOAc solution), EtOH; (c) amino acids, WSCD·HCl, HOBt, solvents.

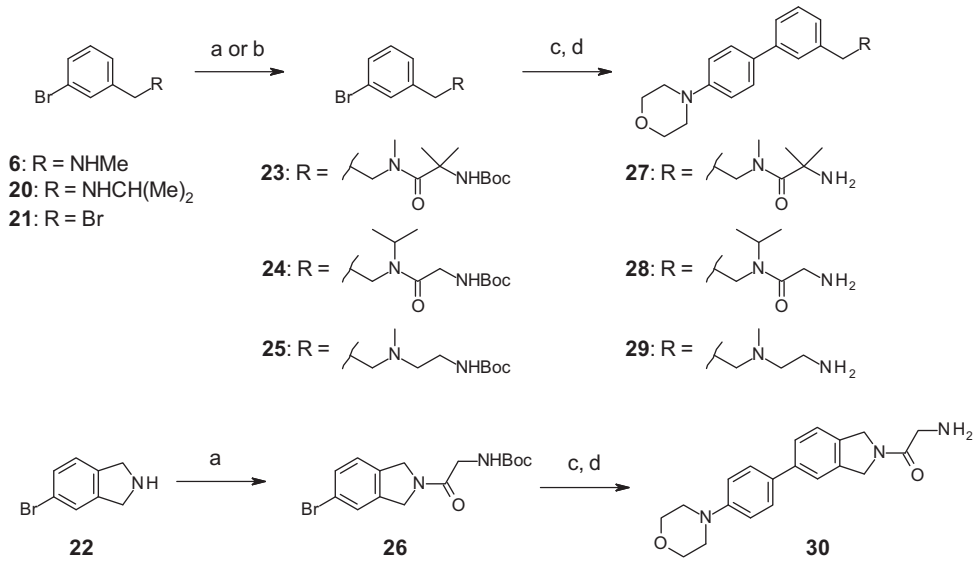

Scheme 5. Reagents and conditions: (a) amino acids, WSCD·HCl, HOBt, CH_2Cl_2; (b) *tert*-butyl [2-(methylamino)ethyl]carbamate, K_2CO_3, DMF; (c) **15**, $Pd(PPh_3)_4$, Na_2CO_3, DME/H_2O, 80–90 °C; (d) 4 M HCl (EtOAc solution), solvents.

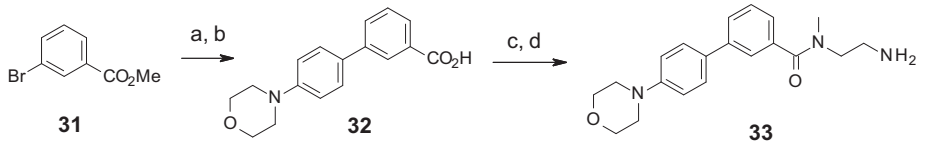

Scheme 6. Reagents and conditions: (a) **15**, $Pd(PPh_3)_4$, Na_2CO_3, DME/H_2O, 80 °C (b) 1 M NaOH aq, EtOH, 60 °C; (c) *tert*-butyl [2-(methylamino)ethyl]carbamate, WSCD·HCl, HOBt, DMF; (d) 4 M HCl (EtOAc solution), MeOH.

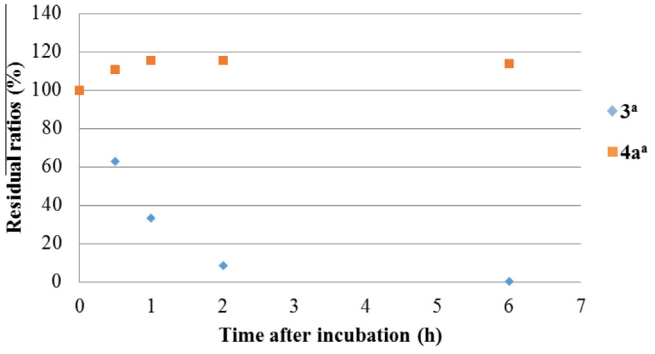

Figure 2. Residual ratios (% to initial concentration) of compound **3** and **4a** after incubation with rat blood ($n = 3$). [a] Hydrochloride salt.

we planned further modification of **4a** in order to increase in vitro potency.

To design more potent VAP-1 inhibitors, we initially performed docking analysis of **4a** with the human VAP-1 model using Inoue's method, as shown in Figure 3.[13] As a starting structure, the primary amine group of **4a** formed a Schiff base intermediate with TPQ. In addition to this covalent interaction of the primary amine group, this model revealed the following three interactions. First, the left phenyl ring of **4a** formed a CH-π interaction with Leu447. Second, the oxygen of the carbonyl group formed a CH-O interaction with Leu468. Third, the hydrogen at the α-position of the carbonyl group formed a CH-O interaction with the Leu468 backbone carbonyl oxygen. Since the glycine amide moiety (right part) and left phenyl ring interact with VAP-1, we considered that the structure of the right part and the spatial relationship between the left phenyl ring and the right part are important for VAP-1 inhibitory activ-

Table 2
In vitro and pharmacodynamic profile of **3** and **4a**

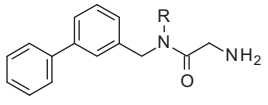

Compound	R	VAP-1 IC_{50} (μM)[a]		Rat ex vivo[b]	
		Human	Rat	Dose (mg/kg, po)	Inhibition ratio (at 1 h) (%)
3[c]	H	0.18	0.023	100	17
4a	Me	0.80	0.12	60	69

[a] IC_{50} values are shown as the mean of independent experiments ($n = 2–3$).
[b] Inhibitory effect on plasma VAP-1 activity in rats ($n = 3–5$) at 1 h after oral administration of compound **3** or **4a**.
[c] Hydrochloride salt.

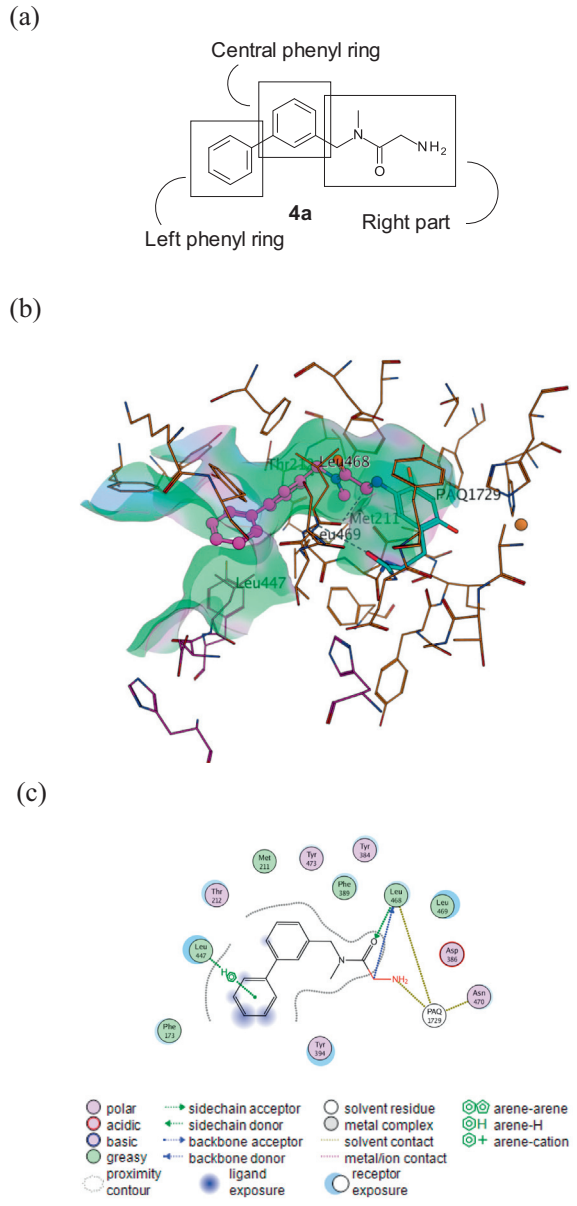

Figure 3. (a) Structure of **4a**. (b) Molecular modeling results for **4a** with human VAP-1. (c) Two-dimensional diagram prepared by the ligand interactions application in MOE.[16b] Arrows indicate interaction.

ity. In addition to these interactions, this molecular modeling predicted that there is limited steric tolerance around the central phenyl ring and right part since these sites are contiguous with amino acid residues such as Leu468, Leu469, Met211, and Thr212. In contrast to the central phenyl ring and right part, considerable space around the 4-position of the left phenyl ring is suggested since this side faces toward the solvent side. The results of docking analysis of **4a** suggested that it is most reasonable to introduce substituents around the 4-position of the left phenyl ring in order to improve VAP-1 inhibitory activity of **4a**.

Based on the results from the docking analysis mentioned above, we introduced chloro group into the 4-position of the left phenyl ring of **4a** (Table 3). Predictably, introduction of chloro group at this position was well tolerated, as 4-chloro derivative **4b** showed 3-fold increased inhibitory activity compared to **4a** with an IC_{50} value of 0.24 μM. In contrast, 3-chloro analog **4c** (IC_{50} = 1.3 μM) and 2-chloro analog **4d** (IC_{50} = 4.1 μM) showed

Table 3
SARs of chloro group substituted derivatives

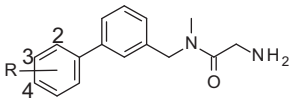

Compound	R	Human VAP-1 IC_{50} (μM)[a]
4a	H	0.80
4b[b]	4-Cl	0.24
4c[c]	3-Cl	1.3
4d[b]	2-Cl	4.1

[a] IC_{50} value is shown as the mean of independent experiments (n = 2–3).
[b] Hydrochloride salt.
[c] Ethanedioate salt.

decreased inhibitory activity compared to **4a**. These SARs suggested that introduction of substituents at the 4-position of the left phenyl ring is optimal for the improvement of VAP-1 inhibitory activities. Based on this result, we next investigated the effect of several substituent groups at the 4-position on the left phenyl ring. Polar substituents were considered for introduction as there are hydrophilic residues like Asp446 and His450 around the solvent side.

Table 4 shows VAP-1 inhibitory activities of compounds having carboxylic acid, amide and urea substituent groups at the 4-position on the left phenyl ring. Introduction of carboxylic acid resulted in a loss of VAP-1 inhibitory activity (**10**), suggesting that anionic groups are not tolerated at this position. While carbamoyl analog **11a** showed 2-fold decreased potency (IC_{50} = 1.6 μM) compared to **4a**, all the other compounds in Table 4 (**11b–11d**, **4e**, and **12a–12b**), which have an amide or urea moiety, exhibited increased inhibitory activity (IC_{50} = 0.083–0.61 μM). In particular, **12b** exhibited the most potent VAP-1 inhibitory activity with an IC_{50} value of 0.083 μM among the compounds we examined. These results were consistent with the results of docking analysis, and suggested that steric hindrance at this position is well tolerated.

Parallel artificial membrane permeability assay (PAMPA) is a commonly used model to predict the permeability of a compound by measuring its flux across an artificial membrane.[15] **11b–11d**, **4e**, and **12a–12b** showed low permeability in PAMPA (P_e - $\leqslant 3.8 \times 10^{-6}$ cm/s). Since these results predicted the possibility of poor membrane permeability of these compounds leading to poor absorption from the small intestine, we considered that it is important to improve permeability in PAMPA. PAMPA value often correlates with topological polar surface area (TPSA),[15b] and compounds in Table 4 tend to show this correlation. TPSA values were calculated using Molecular Operating Environment (MOE).[16b] The values of **11b–11d**, **4e**, and **12a–12b** which showed poor PAMPA values were higher than 60 Å^2, whereas **4a** and **4b** showed good PAMPA values ($P_e > 30 \times 10^{-6}$ cm/s) with lower TPSA value (46.3 Å^2) than 60 Å^2. Thus, we designed a compound with a TPSA value lower than 60 Å^2 to improve permeability in PAMPA.

The results of benzylamine and aniline analogs which have TPSA values lower than 60 Å^2 are summarized in Table 5. Benzylamine derivative **13** showed improved VAP-1 inhibitory activity (IC_{50} = 0.48 μM) compared to **4a**, indicating that introduction of a basic substituent group at this position is also well tolerated. Although dimethylamino analog **4f** showed decreased activity (IC_{50} = 3.0 μM), morpholino analog **4g** and *N*-methyl-piperazino analog **4h** showed improved VAP-1 inhibitory activity (IC_{50} = 0.34 and 0.33 μM, respectively) compared to **4a**. As we expected, **4f** and **4g**, which had TPSA values lower than 60 Å^2 (49.6 and 58.8 Å^2, respectively) showed improved PAMPA values (P_e = 28.1 and 22.1 × 10^{-6} cm/s, respectively). On the other hand, **13** and

Table 4
SARs of 4-substituted derivatives

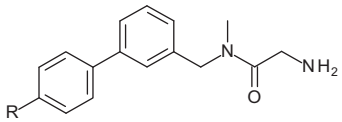

Compound	R	Human VAP-1 IC_{50} (μM)[a]	PAMPA[b], P_e (10^{-6} cm/s) at pH = 6.5	TPSA (Å^2)[c]
4a	H	0.80	>30	46.3
4b[d]	Cl	0.24	>30	46.3
10[d]	HO_2C–	14	NT[g]	83.6
11a[d]	H_2NOC–	1.6	NT[g]	89.4
11b[d]	EtHNOC–	0.61	<0.2	75.4
11c[e]	Et_2NOC–	0.56	3.8	66.6
11d[f]	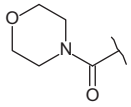	0.42	<0.1	75.9
4e[d]	AcHN–	0.46	<0.2	75.4
12a[e]	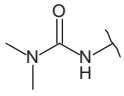	0.28	<0.2	78.7
12b[e]	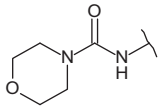	0.083	<0.2	87.9

[a] IC_{50} value is shown as the mean of independent experiments (n = 2–3).
[b] PAMPA Evolution™ (*p*ION Inc., Billerica, MA), donor buffer pH = 6.5.
[c] TPSA values calculated by MOE2014.0901.
[d] Hydrochloride salt.
[e] Ethanedioate salt.
[f] (2*R*,3*R*)-Tartrate salt.
[g] NT = not tested.

Table 5
SARs of benzylamine and aniline derivatives

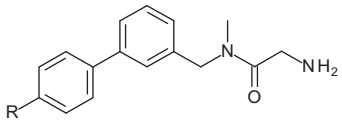

Compound	R	Human VAP-1 IC_{50} (μM)[a]	PAMPA[b], P_e (10^{-6} cm/s) at pH = 6.5	TPSA (Å^2)[c]	pK_a[d]
4a	H	0.80	>30	46.3	–
13[e]	Et_2NH_2C–	0.48	1.0	49.6	9.7
4f[f]	Me_2N–	3.0	28.1	49.6	5.0
4g[f]	Morpholine	0.34	22.1	58.8	5.1
4h[g]		0.33	1.0	52.8	7.8 3.1

[a] IC_{50} value is shown as the mean of independent experiments (n = 2–3).
[b] PAMPA Evolution™ (*p*ION Inc., Billerica, MA), donor buffer pH = 6.5.
[c] TPSA values calculated by MOE2014.0901.
[d] pK_a values other than the primary amine group which were calculated using ACD pK_a prediction software.[17]
[e] Dihydrochloride salt.
[f] Ethanedioate salt.
[g] (2*R*,3*R*)-Tartrate salt.

4h showed poor PAMPA values ($P_e = 1.0 \times 10^{-6}$ cm/s) in spite of having lower TPSA values (49.6 and 52.8 Å^2, respectively) than 60 Å^2. These poor PAMPA values of **13** and **4h** may be due in part to the strong basicity of benzylamine (pK_a = 9.7, calculated using ACD pK_a prediction software[17]) in **13** and *N*-methyl-piperazine (pK_a = 7.8) in **4h**. These results from Table 5 suggested that low TPSA values (lower than 60 Å^2) and weak basicity (lower than 5.1) are both important for high PAMPA values of glycine amide derivatives. Among the compounds examined in Table 5, **4g** exhibited an improvement in in vitro potency with high PAMPA value.

We next investigated the SARs around the right part of **4g** as summarized in Table 6. Conversion of the primary amine group into a secondary amine group (**17**) or tertiary amine group (**18**) resulted in a loss of VAP-1 inhibitory activity. These results suggested that the primary amine group is essential for VAP-1 inhibitory activity. This is consistent with our assumption that the

Table 6
SARs of 4-(biphenyl-4-yl)morpholine derivatives

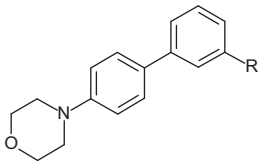

Compound	R or structure	Human VAP-1 IC_{50} (μM)[a]
4g[b]	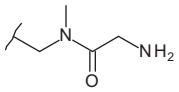	0.34
17[c]	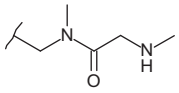	>100
18[c]	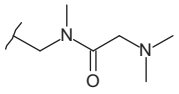	>100
27[c]	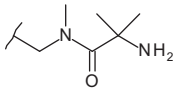	>100
28[c]	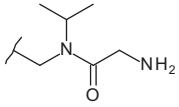	>100
30[d]	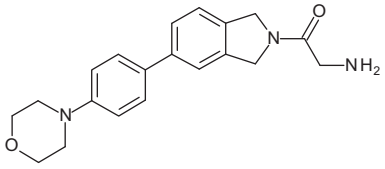	2.0
19[c]	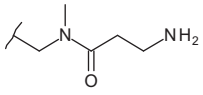	4.0
29[c]	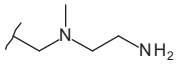	1.8
33[c]	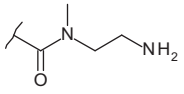	>100

[a] IC_{50} value is shown as the mean of independent experiments ($n = 2$).
[b] Ethanedioate salt.
[c] (2*R*,3*R*)-Tartrate salt
[d] Hydrochloride salt.

primary amine group would form a Shiff base intermediate with TPQ to inhibit VAP-1 activity. **27** (gem-dimethyl derivative) showed no activity, this may be responsible for the difficulty of **27** in forming a Shiff base intermediate with TPQ due to its steric hindrance adjacent to the primary amine group. Introduction of an isopropyl group on the nitrogen atom (**28**) also resulted in a loss of VAP-1 inhibitory activity. This result suggested that steric hindrance around the nitrogen atom is very limited. Isoindoline analog **30** showed 6-fold decreased inhibitory activity compared to **4g**. The reason for this may be that **30** could not interact properly with VAP-1 enzyme due to an altered spatial relationship between the left phenyl ring and right part because of its cyclic structure. Introduction of a longer alkyl chain (**19**) led to deceased VAP-1 inhibitory activity ($IC_{50} = 4.0$ μM), suggesting that length of the alkyl chain between the carbonyl group and primary amine group is also important for VAP-1 inhibitory activity. Removal of the carbonyl group (**29**) and conversion of the position of the carbonyl group (**33**) showed less potent VAP-1 inhibitory activities compared to **4g**, suggesting that the position and existence of the carbonyl group are also important for VAP-1 inhibitory activity. As predicted from the results of docking analysis, these results in Table 6 indicated that conversion of the right part in **4g** while maintaining VAP-1 inhibitory activity is difficult.

The results of docking analysis of **4g** with the human VAP-1 model are shown in Figure 4. The predicted binding mode of **4g** was similar to that of **4a**. Introduction of morpholine at the 4-position of the left phenyl ring might have contributed to increased inhibitory activity due to increased Van der Waals interaction by occupying the solvent site.

The inhibitory activities of **4b** and **4g** against rat VAP-1 were further evaluated using a radiochemical enzyme assay (Table 7). **4b** and **4g** showed more potent rat VAP-1 inhibitory activities with an IC_{50} value of 0.053 μM and 0.036 μM, respectively, compared to **4a** ($IC_{50} = 0.12$ μM). On the basis of enhanced in vitro activity with high PAMPA values ($P_e > 20 \times 10^{-6}$ cm/s), **4b** and **4g** were selected for further evaluation (Table 7). Oral administration of **4b** and **4g** at 10 mg/kg inhibited rat plasma VAP-1 activity by 35% and 92%, respectively. Furthermore, **4g** exhibited a VAP-1 inhibitory effect in rat plasma from lower dose, as oral administration of **4g** at 1 mg/kg inhibited rat plasma VAP-1 activity by 60%. In addition to the improved in vitro potency of **4g**, the reason for the potent ex vivo efficacy of this compound may be explained in part by

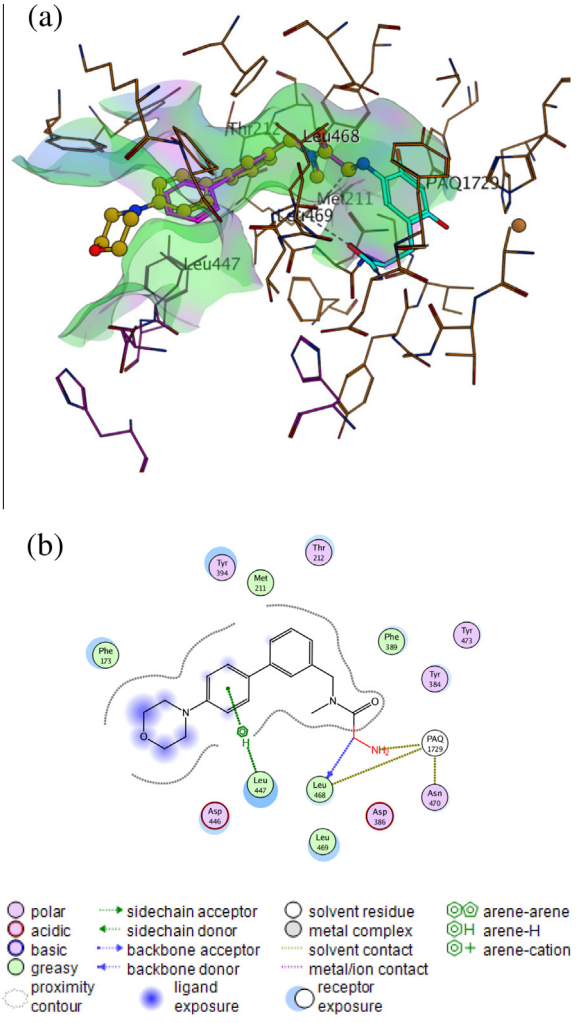

Figure 4. (a) Molecular modeling results for **4a** (pink) and **4g** (yellow, ball and stick) with human VAP-1. (b) Two-dimensional diagram prepared by the ligand interactions application in MOE.[16b] Arrows indicate interaction.

Table 7
Rat VAP-1 inhibitory activities and pharmacodynamic profiles of **4a**, **4b**, and **4g**

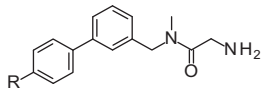

Compound	R	VAP-1 IC_{50} (μM)[a]		Rat ex vivo[b]		$CLogP$[c]
		Human	Rat	Dose (mg/kg, po)	Inhibition ratio (at 1 h) (%)	
4a	H	0.80	0.12	60	69	2.08
4b[d]	Cl	0.24	0.053	10	35	2.65
4g[e]	Morpholine	0.34	0.036	10	92	1.22
				3	87	
				1	60	

[a] IC_{50} values are shown as the mean of independent experiments (n = 2–3).
[b] Inhibitory effect on plasma VAP-1 activity in rats (n = 3–5) at 1 h after oral administration of test compounds.
[c] Log$P$ values calculated using ACD Log$P$ prediction software.[17]
[d] Hydrochloride salt.
[e] Ethanedioate salt.

Table 8
Pharmacokinetic profiles of compound **4g** in rats

Route	AUC_{0-24h} (ng·h/mL)	C_{max} (ng/mL)	CL_{tot} (mL/min/kg)	$t_{1/2}$ (h)	V_{dss} (L/kg)	BA (%)
iv (1 mg/kg)	126.7		133.9	0.47	6.06	
po (1 mg/kg)	69.6	73.4		0.58		54.9

lower plasma protein binding ratio of **4g** (**4a**: 71%, **4b**: 92%, **4g**: 62%) due to its lower lipophilicity ($CLogP$ values; **4a**: 2.08, **4b**: 2.65, **4g**: 1.22, calculated using ACD Log$P$ prediction software[17]), which may lead to a higher unbound plasma concentration of **4g** compared to **4a** and **4b**.

4g showed an acceptable pharmacokinetic profile as shown in Table 8. Plasma C_{max} was 73.4 ng/mL at an oral dose of 1 mg/kg, which is 6 times higher than the IC_{50} value of **4g** (0.036 μM, rat).

4. Conclusion

In summary, we synthesized and evaluated a series of glycine amide derivatives as novel VAP-1 inhibitors, and revealed that the tertiary amide moiety is important for stability in rat blood. Based on the docking analysis, we also found that the 4-position of the left phenyl ring of glycine amide derivatives is an optimal position for introducing substituent groups to increase VAP-1 inhibitory activity. In addition, we found that, for glycine amide derivatives, low TPSA values and weak basicity are both important for good PAMPA values. These findings led to the identification of **4b** (chloro analog) and **4g** (morpholino analog), which had enhanced VAP-1 inhibitory activity while maintaining good PAMPA values. Further, these compounds were subjected to rat ex vivo assay, and **4g** showed the most potent inhibitory effect on rat plasma VAP-1 activity after oral administration. Further studies to identify potent and orally available VAP-1 inhibitors for clinical development are underway.

5. Experimental

5.1. Chemistry

^{1}H NMR spectra were recorded on a Varian VNS-400, JEOL JNM-LA400 or JEOL JNM-AL400 spectrometer. Chemical shifts were expressed in δ values (ppm) using tetramethylsilane as the internal standard (s = singlet, d = doublet, t = triplet, m = multiplet, dd = double doublet, and br = broad peak). Mass spectra (MS) were recorded on a JEOL LX-2000, Waters ZQ-2000 or Waters LCT Premier mass spectrometer. Elemental analyses were conducted using a Yanaco MT-6 (C, H, N), Yanaco JM10 (C, H, N), Elementar Vario EL III (C, H, X), Dionex ICS-3000 (S, halogene), and Dionex DX-500 (S, halogene) and were within ±0.4% of theoretical values. All reactions were carried out using commercially available reagents and solvents without further purification. The following abbreviations are used: AcOH, acetic acid; MeCN, acetonitrile; DCE, 1,2-dichloroethane; DME, 1,2-dimethoxyethane; DMF, *N*,*N*-dimethylformamide; DMSO, *N*,*N*-dimethylsulfoxide; EtOAc, ethyl acetate; EtOH, ethanol; Et_2O, diethyl ether; HOBt, 1-hydroxybenzotriazole; MeOH, methanol; WSCD, 1-ethyl-3-(3′-dimethylaminopropyl) carbodiimide; and Et_3N, triethylamine.

5.1.1. *N*-(Biphenyl-3-ylmethyl)glycinamide hydrochloride (3)

To a solution of 3-phenylbenzylamine (**5**; 190 mg, 1.04 mmol), *N*-(*tert*-butoxycarbonyl)glycine (200 mg, 1.14 mmol) and HOBt (154 mg, 1.14 mmol) in DMF was added WSCD·HCl (219 mg, 1.14 mmol) at room temperature. After being stirred overnight, the mixture was concentrated in vacuo. The residue was diluted with EtOAc and the mixture was washed with 0.5 M HCl aqueous solution, 1 M $NaHCO_3$ aqueous solution, and brine. The organic layer was dried over $MgSO_4$ and concentrated in vacuo to give the solid. This solid was dissolved in 4 M HCl/EtOAc at room temperature. After being stirred for 1 h, the mixture was concentrated in vacuo. The residue was triturated with Et_2O and filtered to give the product (285 mg, 99%) as a solid. ^{1}H NMR (DMSO-d_6) δ 3.63 (2H, s), 4.43 (2H, d, J = 5.8 Hz), 7.30 (1H, d, J = 7.8 Hz), 7.35–7.51 (4H, m), 7.54–7.62 (2H, m), 7.64–7.69 (2H, m), 8.18 (3H, br s), 9.02 (1H, t, J = 5.6 Hz); MS (ESI) m/z $[M+H]^+$ 241; Anal. Calcd for $C_{15}H_{16}N_2O{\cdot}HCl{\cdot}0.2H_2O$: C, 64.26; H, 6.26; N, 9.99; Cl, 12.64. Found: C, 64.47; H, 6.21; N, 10.14; Cl, 12.43.

5.1.2. *tert*-Butyl {2-[(3-bromobenzyl)(methyl)amino]-2-oxoethyl}carbamate (7)

To a solution of 1-(3-bromophenyl)-*N*-methylmethanamine (6; 45.6 g, 228 mmol) in CH_2Cl_2 (700 mL) were added *N*-(*tert*-butoxycarbonyl)glycine (43.9 g, 251 mmol), WSCD·HCl (52.4 g, 274 mmol), and HOBt (37.1 g, 275 mmol). After being stirred at

room temperature for 1 week, the mixture was diluted with water and the mixture was extracted with $CHCl_3$. The organic layer was washed with saturated $NaHCO_3$ aqueous solution and brine, dried over Na_2SO_4, and concentrated in vacuo. The residue was purified by column chromatography on silica gel (hexane/EtOAc = 7:1 to 1:1) to give the product (49.1 g, 60%) as an oil. ^{1}H NMR ($CDCl_3$): this compound exists as a pair of rotamers at room temperature. δ 1.44 (minor rotamer, 9H, s), 1.46 (major rotamer, 9H, s), 2.90 (major rotamer, 3H, s), 2.98 (minor rotamer, 3H, s), 3.96–4.06 (2H, m), 4.44 (minor rotamer, 2H, s), 4.57 (major rotamer, 2H, s), 5.54 (1H, br s), 7.06–7.25 (2H, m), 7.28–7.49 (2H, m); MS (ESI) m/z $[M+H]^+$ 357, 359.

5.1.3. *N*-(Biphenyl-3-ylmethyl)-*N*-methylglycinamide (4a)

To a mixture of **7** (215 mg, 0.60 mmol) in dioxane (4.0 mL)/water (1.0 mL) were added phenylboronic acid (110 mg, 0.90 mmol), Na_2CO_3 (200 mg, 1.89 mmol), and $Pd(PPh_3)_4$ (33 mg, 0.029 mmol) under an argon atmosphere. The mixture was stirred at 80 °C for 16 h. After being cooled to room temperature, the mixture was diluted with water and extracted with EtOAc. The organic layer was dried over $MgSO_4$ and concentrated in vacuo. The residue was purified by column chromatography on silica gel (hexane/EtOAc = 98:2 to 2:1) to afford *tert*-butyl {2-[(biphenyl-3-ylmethyl)(methyl)amino]-2-oxoethyl}carbamate. To a solution of *tert*-butyl {2-[(biphenyl-3-ylmethyl)(methyl)amino]-2-oxoethyl}-carbamate in EtOAc (3.0 mL) was added 4 M HCl/EtOAc (2.00 mL, 8.00 mmol). After being stirred at room temperature for 2 h, the resulting precipitate was filtered to give *N*-(Biphenyl-3-ylmethyl)-*N*-methylglycinamide hydrochloride (146 mg, 83%) as a colorless solid. ^{1}H NMR (DMSO-d_6): this compound exists as a pair of rotamers at room temperature. δ 2.91 (minor rotamer, 3H, s), 2.97 (major rotamer, 3H, s), 3.91 (minor rotamer, 2H, s), 3.96 (major rotamer, 2H, s), 4.63 (minor rotamer, 2H, s), 4.64 (major rotamer, 2H, s), 7.24–7.29 (1H, m), 7.36–7.42 (1H, m), 7.42–7.51 (3H, m), 7.52–7.70 (4H, m), 8.16 (3H, br s); MS (ESI) m/z $[M+H]^+$ 255; Anal. Calcd for $C_{16}H_{18}N_2O{\cdot}HCl$: C, 66.09; H, 6.59; N, 9.63; Cl, 12.19. Found: C, 66.10; H, 6.63; N, 9.60; Cl, 11.96.

To a solution of *N*-(Biphenyl-3-ylmethyl)-*N*-methylglycinamide hydrochloride (240 mg, 0.83 mmol) in water (5.0 mL) was added 1 M $NaHCO_3$ aqueous solution until pH = 8. The mixture was extracted with $CHCl_3$. The organic layer was washed with brine and concentrated in vacuo to give the product (200 mg, 95%) as a solid. ^{1}H NMR (DMSO-d_6): this compound exists as a pair of rotamers at room temperature. δ 1.74 (2H, br s), 2.87 (minor rotamer, 3H, s), 2.89 (major rotamer, 3H, s), 3.40 (2H, s), 4.58 (minor rotamer, 2H, s), 4.59 (major rotamer, 2H, s), 7.17–7.26 (1H, m), 7.35–7.52 (5H, m), 7.52–7.59 (1H, m), 7.62–7.67 (2H, m); MS (FAB) m/z $[M+H]^+$ 255.

5.1.4. *N*-[(4′-Chlorobiphenyl-3-yl)methyl]-*N*-methylglycinamide hydrochloride (4b)

Compound **4b** was prepared from **7** and (4-chlorophenyl)boronic acid in 75% yield as a colorless solid, using a similar approach to that described for **4a·HCl**. ^{1}H NMR (DMSO-d_6): this compound exists as a pair of rotamers at room temperature. δ 2.90 (minor rotamer, 3H, s), 2.97 (major rotamer, 3H, s), 3.90 (minor rotamer, 2H, s), 3.96 (major rotamer, 2H, s), 4.63 (minor rotamer, 2H, s), 4.64 (major rotamer, 2H, s), 7.24–7.34 (1H, m), 7.44–7.64 (5H, m), 7.67–7.80 (2H, m), 8.30 (3H, br s); MS (FAB) m/z $[M+H]^+$ 289; Anal. Calcd for $C_{16}H_{17}ClN_2O{\cdot}HCl$: C, 59.09; H, 5.58; N, 8.61; Cl, 21.80. Found: C, 59.08; H, 5.61; N, 8.61; Cl, 21.75.

5.1.5. *N*-[(3′-Chlorobiphenyl-3-yl)methyl]-*N*-methylglycinamide ethanedioate (4c)

To a mixture of **7** (293 mg, 0.82 mmol) in toluene (4.0 mL)/water (2.0 mL) were added (3-chlorophenyl)boronic acid (192 mg, 1.23 mmol), Na_2CO_3 (174 mg, 1.64 mmol), and $Pd(PPh_3)_4$ (28 mg, 0.025 mmol). The mixture was stirred at 80 °C overnight. After being cooled to room temperature, the mixture was diluted with water and extracted with EtOAc. The organic layer was dried over $MgSO_4$ and concentrated in vacuo. The residue was purified by column chromatography on silica gel (hexane/EtOAc = 1:0 to 1:2) to afford *tert*-butyl (2-{[(3′-chlorobiphenyl-3-yl)methyl](methyl)amino}-2-oxoethyl)carbamate. To a solution of *tert*-butyl (2-{[(3′-chlorobiphenyl-3-yl)methyl](methyl)amino}-2-oxoethyl)carbamate in EtOAc (5.0 mL) was added 4 M HCl/EtOAc (10.0 mL, 40.0 mmol). After being stirred at room temperature for 2 h, the mixture was concentrated in vacuo. The residue was diluted with saturated $NaHCO_3$ aqueous solution and the mixture was extracted with $CHCl_3$. The organic layer was dried over Na_2SO_4 and concentrated in vacuo. To a solution of the residue in EtOH was added oxalic acid (74 mg, 0.82 mmol). The mixture was concentrated in vacuo to give the product (186 mg, 60%) as a colorless solid. ^{1}H NMR (DMSO-d_6): this compound exists as a pair of rotamers at room temperature. δ 2.90 (minor rotamer, 3H, s), 2.96 (major rotamer, 3H, s), 3.93 (minor rotamer, 2H, s), 3.96 (major rotamer, 2H, s), 4.61 (minor rotamer, 2H, s), 4.64 (major rotamer, 2H, s), 7.27–7.34 (1H, m), 7.44–7.67 (6H, m), 7.71 (major rotamer, 1H, dd J = 1.8, 1.8 Hz), 7.74 (minor rotamer, 1H, dd J = 1.8, 1.8 Hz); MS (FAB) m/z $[M+H]^+$ 289; Anal. Calcd for $C_{16}H_{17}ClN_2O{\cdot}C_2H_2O_4$: C, 57.07; H, 5.06; N, 7.40; Cl, 9.36. Found: C, 57.03; H, 5.04; N, 7.37; Cl, 9.40.

5.1.6. *N*-[(2′-Chlorobiphenyl-3-yl)methyl]-*N*-methylglycinamide hydrochloride (4d)

Compound **4d** was prepared from **7** and (2-chlorophenyl)boronic acid in 73% yield as a colorless solid, using a similar approach to that described for **4a·HCl**. ^{1}H NMR (DMSO-d_6): this compound exists as a pair of rotamers at room temperature. δ 2.91 (minor rotamer, 3H, s), 2.96 (major rotamer, 3H, s), 3.88 (minor rotamer, 2H, s), 3.94 (major rotamer, 2H, s), 4.63 (2H, s), 7.28–7.53 (7H, m), 7.56–7.60 (1H, m), 8.23 (3H, br s); MS (FAB) m/z $[M+H]^+$ 289; Anal. Calcd for $C_{16}H_{17}ClN_2O{\cdot}HCl$: C, 59.09; H, 5.58; N, 8.61; Cl, 21.80. Found: C, 59.08; H, 5.62; N, 8.67; Cl, 21.65.

5.1.7. *N*-[(4′-Acetamidobiphenyl-3-yl)methyl]-*N*-methylglycinamide hydrochloride (4e)

Compound **4e** was prepared from **7** and (4-acetamidophenyl) boronic acid in 89% yield as a colorless solid, using a similar approach to that described for **4a·HCl**. ^{1}H NMR (DMSO-d_6): this compound exists as a pair of rotamers at room temperature. δ 2.07 (3H, s), 2.91 (minor rotamer, 3H, s), 2.96 (major rotamer, 3H, s), 3.88–4.01 (2H, m), 4.61 (minor rotamer, 2H, s), 4.63 (major rotamer, 2H, s), 7.18–7.28 (1H, m), 7.39–7.64 (5H, m), 7.66–7.74 (2H, m), 8.22 (3H, br s), 10.19 (1H, s); MS (ESI) m/z $[M+H]^+$ 312; Anal. Calcd for $C_{18}H_{21}N_3O_2{\cdot}1.1HCl{\cdot}1.5H_2O$: C, 57.12; H, 6.68; N, 11.10; Cl, 10.30. Found: C, 57.17; H, 6.68; N, 11.26; Cl, 10.41.

5.1.8. *N*-{[4′-(Dimethylamino)biphenyl-3-yl]methyl}-*N*-methylglycinamide ethanedioate (4f)

Compound **4f** was prepared from **7** and [4-(dimethylamino) phenyl]boronic acid in 75% yield as a colorless solid, using a similar approach to that described for **4c**. ^{1}H NMR (DMSO-d_6): this compound exists as a pair of rotamers at room temperature. δ 2.89 (minor rotamer, 3H, s), 2.93 (major rotamer, 3H, s), 2.94 (6H, s), 3.73 (minor rotamer, 2H, s), 3.79 (major rotamer, 2H, s), 4.57 (minor rotamer, 2H, s), 4.59 (major rotamer, 2H, s), 6.77–6.83 (2H, m), 7.07–7.15 (1H, m), 7.34–7.58 (5H, m); MS (ESI) m/z $[M+H]^+$ 298; HRMS (ESI) m/z Calcd for $C_{18}H_{24}N_3O$ $[M+H]^+$: 298.1914. Found: 298.1916.

5.1.9. *N*-Methyl-*N*-{[4′-(morpholin-4-yl)biphenyl-3-yl]methyl} glycinamide ethanedioate (4g)

Compound **4g** was prepared from **7** and 4-[4-(4,4,5,5-tetramethyl-1,3,2-dioxaborolan-2-yl)phenyl]morpholine in 72% yield as a colorless solid, using a similar approach to that described for **4c**. ^{1}H NMR (DMSO-d_6): this compound exists as a pair of rotamers at room temperature. δ 2.90 (minor rotamer, 3H, s), 2.95 (major rotamer, 3H, s), 3.10–3.21 (4H, m), 3.70–3.82 (4H, m), 3.93 (minor rotamer, 2H, s), 3.96 (major rotamer, 2H, s), 4.59 (minor rotamer, 2H, s), 4.61 (major rotamer, 2H, s), 6.99–7.06 (2H, m), 7.10–7.24 (1H, m), 7.36–7.60 (5H, m), 7.92 (2H, br s); MS (ESI) m/z [M+H]$^+$ 340; Anal. Calcd for $C_{20}H_{25}N_3O_2{\cdot}C_2H_2O_4$: C, 61.53; H, 6.34; N, 9.78. Found: C, 61.28; H, 6.35; N, 9.75.

5.1.10. *N*-Methyl-*N*-{[4′-(4-methylpiperazin-1-yl)biphenyl-3-yl] methyl}glycinamide (2*R*,3*R*)-tartrate (4h)

Compound **4h** was prepared from **7** and 1-methyl-4-[4-(4,4,5,5-tetramethyl-1,3,2-dioxaborolan-2-yl)phenyl]piperazine in 68% yield as a colorless solid, using a similar approach to that described for **4c**. ^{1}H NMR (DMSO-d_6): this compound exists as a pair of rotamers at room temperature. δ 2.25 (3H, s), 2.46–2.52 (4H, m), 2.90 (minor rotamer, 3H, s), 2.94 (major rotamer, 3H, s), 3.15–3.23 (4H, m), 3.86 (2H, tartaric acid), 3.87 (minor rotamer, 2H, s), 3.92 (major rotamer, 2H, s), 4.58 (minor rotamer, 2H, s), 4.61 (major rotamer, 2H, s), 6.99–7.06 (2H, m), 7.13–7.18 (1H, m), 7.36–7.58 (5H, m); MS (ESI) m/z [M+H]$^+$ 353; Anal. Calcd for $C_{21}H_{28}N_4O{\cdot}C_4H_6O_6{\cdot}1.7H_2O$: C, 56.32; H, 7.07; N, 10.51. Found: C, 56.37; H, 7.18; N, 10.47.

5.1.11. Methyl 3′-({[*N*-(*tert*-Butoxycarbonyl)glycyl](methyl) amino}methyl)biphenyl-4-carboxylate (8a)

To a mixture of **7** (2.00 g, 5.60 mmol) in DME (30 mL)/EtOH (5.0 mL)/water (10 mL) were added [4-(methoxycarbonyl)phenyl]boronic acid (1.51 g, 8.40 mmol), Na_2CO_3 (1.78 g, 16.8 mmol), and $Pd(PPh_3)_4$ (194 mg, 0.168 mmol). The mixture was stirred at 80 °C overnight. After being cooled to room temperature, the mixture was diluted with water and extracted with $CHCl_3$. The organic layer was dried over $MgSO_4$ and concentrated in vacuo. The residue was purified by column chromatography on silica gel (hexane/EtOAc = 1:0 to 1:2) to give the product (1.99 g, 86%) as a yellow solid. ^{1}H NMR (DMSO-d_6): this compound exists as a pair of rotamers at room temperature. δ 1.37 (minor rotamer, 9H, s), 1.39 (major rotamer, 9H, s), 2.83 (minor rotamer, 3H, s), 2.94 (major rotamer, 3H, s), 3.81–3.95 (5H, m), 4.59 (major rotamer, 2H, s), 4.64 (minor rotamer, 2H, s), 6.83 (major rotamer, 1H, dd, J = 5.7, 5.7 Hz), 6.92 (minor rotamer, 1H, dd, J = 5.8, 5.8 Hz), 7.25–7.35 (1H, m), 7.47 (major rotamer, 1H, dd, J = 7.7, 7.7 Hz), 7.52 (minor rotamer, 1H, dd, J = 7.7, 7.7 Hz), 7.57–7.71 (2H, m), 7.83 (major rotamer, 2H, d, J = 8.4 Hz), 7.89 (minor rotamer, 2H, d, J = 8.4 Hz), 8.04 (2H, d, J = 8.4 Hz); MS (ESI) m/z [M+H]$^+$ 413.

5.1.12. *tert*-Butyl (2-{[(4′-aminobiphenyl-3-yl)methyl](methyl) amino}-2-oxoethyl)carbamate (8b)

Compound **8b** was prepared from **7** and 4-(4,4,5,5-tetramethyl-1,3,2-dioxaborolan-2-yl)aniline in 84% yield as a pale brown solid, using a similar approach to that described for **8a**. ^{1}H NMR (DMSO-d_6): this compound exists as a pair of rotamers at room temperature. δ 1.38 (minor rotamer, 9H, s), 1.40 (major rotamer, 9H, s), 2.82 (major rotamer, 3H, s), 2.91 (minor rotamer, 3H, s), 3.85 (2H, d, J = 5.7 Hz), 4.53 (major rotamer, 2H, s), 4.57 (minor rotamer, 2H, s), 5.22 (2H, br s), 6.63 (2H, d, J = 8.4 Hz), 6.80 (major rotamer, 1H, dd, J = 5.7, 5.7 Hz), 6.87 (minor rotamer, 1H, dd, J = 5.8, 5.8 Hz), 7.05 (1H, d, J = 7.3 Hz), 7.28–7.50 (5H, m); MS (ESI) m/z [M+H]$^+$ 370.

5.1.13. *tert*-Butyl (2-{[(4′-formylbiphenyl-3-yl)methyl](methyl) amino}-2-oxoethyl)carbamate (8c)

Compound **8c** was prepared from **7** and (4-formylphenyl)boronic acid in 89% yield as a beige solid, using a similar approach to that described for **8a**. ^{1}H NMR (DMSO-d_6): this compound exists as a pair of rotamers at room temperature. δ 1.38 (minor rotamer, 9H, s), 1.39 (major rotamer, 9H, s), 2.84 (minor rotamer, 3H, s), 2.95 (major rotamer, 3H, s), 3.87 (2H, d, J = 5.8 Hz), 4.60 (major rotamer, 2H, s), 4.64 (minor rotamer, 2H, s), 6.83 (major rotamer, 1H, dd, J = 5.8, 5.8 Hz), 6.93 (minor rotamer, 1H, dd, J = 5.8, 5.8 Hz), 7.26–7.34 (1H, m), 7.48 (major rotamer, 1H, dd, J = 7.6, 7.6 Hz), 7.54 (minor rotamer, 1H, dd, J = 7.6, 7.6 Hz), 7.60–7.73 (2H, m), 7.89–8.03 (4H, m), 10.06 (1H, s); MS (FAB) m/z [M+H]$^+$ 383.

5.1.14. 3′-({[*N*-(*tert*-Butoxycarbonyl)glycyl](methyl)amino} methyl)biphenyl-4-carboxylic acid (9)

To a solution of **8a** (1.96 g, 4.76 mmol) in MeOH (20 mL) was added 1 M NaOH aqueous solution (14.3 mL, 14.3 mmol). After being stirred at room temperature overnight, 1 M HCl aqueous solution (14.3 mL, 14.3 mmol) was added and the mixture was concentrated in vacuo. The residue was diluted with water and the mixture was extracted with $CHCl_3$. The organic layer was dried over $MgSO_4$, and concentrated in vacuo to give the product (1.93 g, quantitative yield) as a yellow solid. ^{1}H NMR (DMSO-d_6): this compound exists as a pair of rotamers at room temperature. δ 1.38 (minor rotamer, 9H, s), 1.40 (major rotamer, 9H, s), 2.83 (minor rotamer, 3H, s), 2.95 (major rotamer, 3H, s), 3.87 (2H, d, J = 5.7 Hz), 4.59 (major rotamer, 2H, s), 4.64 (minor rotamer, 2H, s), 6.84 (major rotamer, 1H, dd, J = 5.8, 5.8 Hz), 6.93 (minor rotamer, 1H, dd, J = 5.8, 5.8 Hz), 7.24–7.33 (1H, m), 7.46 (major rotamer, 1H, dd, J = 7.6, 7.6 Hz), 7.52 (minor rotamer, 1H, dd, J = 7.6, 7.6 Hz), 7.55–7.70 (2H, m), 7.80 (major rotamer, 2H, d, J = 8.0 Hz), 7.87 (minor rotamer, 2H, d, J = 8.0 Hz), 8.02 (2H, d, J = 8.1 Hz), 13.0 (1H, br s); MS (ESI) m/z [M+H]$^+$ 399.

5.1.15. 3′-{[Glycyl(methyl)amino]methyl}biphenyl-4-carboxylic acid hydrochloride (10)

The mixture of **8a** (167 mg, 0.40 mmol) and 6 M HCl aqueous solution (5.00 mL, 30.0 mmol) was stirred at 100 °C for 2 h. After being cooled to room temperature, the mixture was concentrated in vacuo. To the residue were added EtOH and water, and the resulting precipitate was filtered to give the product (107 mg, 79%) as a colorless solid. ^{1}H NMR (DMSO-d_6): this compound exists as a pair of rotamers at room temperature. δ 2.91 (minor rotamer, 3H, s), 2.97 (major rotamer, 3H, s), 3.92 (minor rotamer, 2H, s), 3.97 (major rotamer, 2H, s), 4.63 (minor rotamer, 2H, s), 4.65 (major rotamer, 2H, s), 7.29–7.35 (1H, m), 7.49 (major rotamer, 1H, dd, J = 7.7, 7.7 Hz), 7.54 (minor rotamer, 1H, dd, J = 7.7, 7.7 Hz), 7.56–7.72 (2H, m), 7.76–7.84 (2H, m), 8.01–8.06 (2H, m), 8.12 (3H, br s); MS (ESI) m/z [M+H]$^+$ 299; Anal. Calcd for $C_{17}H_{18}N_2O_3{\cdot}HCl{\cdot}0.3H_2O$: C, 60.02; H, 5.81; N, 8.23; Cl, 10.42. Found: C, 59.98; H, 5.75; N, 8.26; Cl, 10.48.

5.1.16. 3′-{[Glycyl(methyl)amino]methyl}biphenyl-4-carboxamide hydrochloride (11a)

Compound **11a** was prepared from **9** and ammonium hydroxide in 48% yield as a colorless solid, using a similar approach to that described for **3**. ^{1}H NMR (DMSO-d_6): this compound exists as a pair of rotamers at room temperature. δ 2.91 (minor rotamer, 3H, s), 2.97 (major rotamer, 3H, s), 3.92 (minor rotamer, 2H, s), 3.97 (major rotamer, 2H, s), 4.63 (minor rotamer, 2H, s), 4.65 (major rotamer, 2H, s), 7.27–7.34 (1H, m), 7.41 (1H, br s), 7.47 (major rotamer, 1H, dd, J = 7.7, 7.7 Hz), 7.53 (minor rotamer, 1H, dd, J = 7.7, 7.7 Hz), 7.55–7.71 (2H, m), 7.72–7.79 (2H, m), 7.98 (major rotamer,

2H, d, J = 8.5 Hz), 7.99 (minor rotamer, 2H, d, J = 8.4 Hz), 8.06 (1H, br s), 8.17 (3H, br s); MS (ESI) m/z $[M+H]^+$ 298; Anal. Calcd for $C_{17}H_{19}N_3O_2$·HCl: C, 61.17; H, 6.04; N, 12.59; Cl, 10.62. Found: C, 60.97; H, 6.08; N, 12.50; Cl, 10.59.

5.1.17. *N*-Ethyl-3′-{[glycyl(methyl)amino]methyl}biphenyl-4-carboxamide hydrochloride (11b)

Compound **11b** was prepared from **9** and ethylamine in 44% yield as a colorless solid, using a similar approach to that described for **3**. ^{1}H NMR (DMSO-d_6): this compound exists as a pair of rotamers at room temperature. δ 1.14 (3H, t, J = 7.2 Hz), 2.91 (minor rotamer, 3H, s), 2.97 (major rotamer, 3H, s), 3.27–3.32 (2H, m), 3.92 (minor rotamer, 2H, s), 3.97 (major rotamer, 2H, s), 4.63 (minor rotamer, 2H, s), 4.65 (major rotamer, 2H, s), 7.27–7.33 (1H, m), 7.47 (major rotamer, 1H, dd, J = 7.7, 7.7 Hz), 7.53 (minor rotamer, 1H, dd, J = 7.7, 7.7 Hz), 7.55–7.70 (2H, m), 7.72–7.80 (2H, m), 7.95 (major rotamer, 2H, d, J = 8.4 Hz), 7.96 (minor rotamer, 2H, d, J = 8.4 Hz), 8.16 (3H, br s), 8.56 (1H, t, J = 5.4 Hz); MS (ESI) m/z $[M+H]^+$ 326; Anal. Calcd for $C_{19}H_{23}N_3O_2$·HCl: C, 63.06; H, 6.68; N, 11.61; Cl, 9.80. Found: C, 62.96; H, 6.70; N, 11.57; Cl, 9.81.

5.1.18. *N*,*N*-Diethyl-3′-{[glycyl(methyl)amino]methyl}biphenyl-4-carboxamide ethanedioate (11c)

To a solution of **9** (210 mg, 0.53 mmol) in DMF (5.0 mL) were added *N*-ethylethanamine (42 mg, 0.58 mmol), WSCD (90 mg, 0.58 mmol), HOBt (78 mg, 0.58 mmol) and Et_3N (80 μL, 0.58 mmol) at room temperature. After being stirred at the same temperature overnight, the mixture was concentrated in vacuo. The residue was diluted with water and the mixture was extracted with EtOAc. The organic layer was dried over $MgSO_4$, and concentrated in vacuo. The residue was purified by column chromatography on silica gel (hexane/EtOAc = 1:0 to 3:7) to give *tert*-butyl {2-[{[4′-(diethylcarbamoyl)biphenyl-3-yl]methyl}(methyl)amino]-2-oxoethyl}carbamate. To a solution of *tert*-butyl {2-[{[4′-(diethylcarbamoyl)biphenyl-3-yl]methyl}(methyl)amino]-2-oxoethyl}carbamate in EtOH (10 mL) was added 4 M HCl/EtOAc (10.0 mL, 40.0 mmol). After being stirred at room temperature for 2 h, the mixture was concentrated in vacuo. The residue was diluted with saturated $NaHCO_3$ aqueous solution, and the mixture was extracted with $CHCl_3$. The organic layer was dried over Na_2SO_4, and concentrated in vacuo. To a solution of the residue in EtOH was added oxalic acid (47 mg, 0.53 mmol). The mixture was concentrated in vacuo. To the residue were added EtOH and water, and the resulting precipitate was filtered to give the product (90 mg, 39%) as a colorless solid. ^{1}H NMR (DMSO-d_6): this compound exists as a pair of rotamers at room temperature. δ 1.00–1.24 (6H, br m), 2.91 (minor rotamer, 3H, s), 2.96 (major rotamer, 3H, s), 3.12–3.55 (4H, br m), 3.94 (minor rotamer, 2H, s), 3.97 (major rotamer, 2H, s), 4.62 (minor rotamer, 2H, s), 4.65 (major rotamer, 2H, s), 7.27–7.33 (1H, m), 7.40–7.53 (3H, m), 7.53–7.69 (2H, m), 7.69–7.78 (2H, m); MS (FAB) m/z $[M+H]^+$ 354; Anal. Calcd for $C_{21}H_{27}N_3O_2·C_2H_2O_4$: C, 62.29; H, 6.59; N, 9.47. Found: C, 62.03; H, 6.55; N, 9.54.

5.1.19. *N*-Methyl-*N*-{[4′-(morpholin-4-ylcarbonyl)biphenyl-3-yl]methyl}glycinamide (2*R*,3*R*)-tartrate (11d)

Compound **11d** was prepared from **9** and morpholine in 71% yield as a colorless solid, using a similar approach to that described for **11c**. ^{1}H NMR (DMSO-d_6): this compound exists as a pair of rotamers at room temperature. δ 2.89 (minor rotamer, 3H, s), 2.93 (major rotamer, 3H, s), 3.31–3.71 (8H, m), 3.68 (minor rotamer, 2H, s), 3.74 (major rotamer, 2H, s), 3.77 (2H, s, tartaric acid), 4.60 (minor rotamer, 2H, s), 4.63 (major rotamer, 2H, s), 7.23–7.32 (1H, m), 7.44–7.68 (5H, m), 7.69–7.76 (2H, m); MS (ESI) m/z $[M+H]^+$ 368; HRMS (ESI) m/z Calcd for $C_{21}H_{26}N_3O$ $[M+H]^+$: 368.1969. Found: 368.1971.

5.1.20. *N*-({4′-[(Dimethylcarbamoyl)amino]biphenyl-3-yl}methyl)-*N*-methylglycinamide ethanedioate (12a)

To a mixture of **8b** (200 mg, 0.54 mmol) in CH_2Cl_2 (6.0 mL) were added pyridine (66 μL, 0.81 mmol) and dimethylcarbamic chloride (55 μL, 0.60 mmol). After being stirred at room temperature for 1 h, the mixture was diluted with water and extracted with $CHCl_3$. The organic layer was dried over $MgSO_4$, and concentrated in vacuo. The residue was purified by column chromatography on silica gel ($CHCl_3$/MeOH = 98/2) to afford *tert*-butyl {2-[({4′-[(dimethylcarbamoyl)amino]biphenyl-3-yl}methyl)(methyl)amino]-2-oxoethyl}carbamate (220 mg, 92%) as a colorless oil. To a solution of *tert*-butyl {2-[({4′-[(dimethylcarbamoyl)amino]biphenyl-3-yl}methyl)(methyl)amino]-2-oxoethyl}carbamate (210 mg, 0.48 mmol) in MeOH was added 4 M HCl/EtOAc (1.20 mL, 4.80 mmol). After being stirred at room temperature for 4 h, the mixture was concentrated in vacuo. The residue was diluted with saturated $NaHCO_3$ aqueous solution, and the mixture was extracted with $CHCl_3$. The organic layer was dried over $MgSO_4$ and concentrated in vacuo. To a solution of the residue in EtOH was added oxalic acid (43 mg, 0.48 mmol). The resulting precipitate was filtered to give the product (125 mg, 61%) as a colorless solid. ^{1}H NMR (DMSO-d_6): this compound exists as a pair of rotamers at room temperature. δ 2.90 (minor rotamer, 3H, s), 2.94 (major rotamer, 3H, s), 2.94 (6H, s), 3.85 (minor rotamer, 2H, s), 3.89 (major rotamer, 2H, s), 4.59 (minor rotamer, 2H, s), 4.61 (major rotamer, 2H, s), 7.15–7.22 (1H, m), 7.33–7.48 (2H, m), 7.48–7.61 (5H, m), 8.43 (1H, br s); MS (ESI) m/z $[M+H]^+$ 341; HRMS (ESI) m/z Calcd for $C_{19}H_{25}N_4O_2$ $[M+H]^+$: 341.1972. Found: 341.1974.

5.1.21. *N*-(3′-{[Glycyl(methyl)amino]methyl}biphenyl-4-yl)morpholine-4-carboxamide ethanedioate (12b)

Compound **12b** was prepared from **8b** and morpholine-4-carbonyl chloride and Et_3N instead of pyridine in 57% yield as a solid, using a similar approach to that described for **12a**. ^{1}H NMR (DMSO-d_6): this compound exists as a pair of rotamers at room temperature. δ 2.91 (minor rotamer, 3H, s), 2.95 (major rotamer, 3H, s), 3.40–3.49 (4H, m), 3.57–3.66 (4H, m), 3.92 (minor rotamer, 2H, s), 3.96 (major rotamer, 2H, s), 4.60 (minor rotamer, 2H, s), 4.62 (major rotamer, 2H, s), 7.17–7.23 (1H, m), 7.38–7.60 (7H, m), 8.67 (major rotamer, 1H, s), 8.68 (minor rotamer, 1H, s); MS (ESI) m/z $[M+H]^+$ 383; Anal. Calcd for $C_{21}H_{26}N_4O_3·C_2H_2O_4·0.7H_2O$: C, 56.95; H, 6.11; N, 11.55. Found: C, 56.88; H, 6.14; N, 11.57.

5.1.22. *N*-({4′-[(Diethylamino)methyl]biphenyl-3-yl}methyl)-*N*-methylglycinamide dihydrochloride (13)

To a solution of **8c** (250 mg, 0.65 mmol) in DCE (5.0 mL) were added diethylamine (205 μL, 1.96 mmol) and AcOH (187 μL, 3.27 mmol). After being stirred at room temperature for 1 h, sodium triacetoxyborohydride (416 mg, 1.96 mmol) was added. After being stirred at room temperature for 1 h, the mixture was diluted with saturated $NaHCO_3$ aqueous solution and extracted with $CHCl_3$. The organic layer was concentrated in vacuo. The residue was purified by column chromatography on amino silica gel (hexane/EtOAc = 1:0 to 1:4) to afford *tert*-butyl {2-[({4′-[(diethylamino)methyl]biphenyl-3-yl}methyl)(methyl)amino]-2-oxoethyl}carbamate. To a solution of *tert*-butyl {2-[({4′-[(diethylamino)methyl]biphenyl-3-yl}methyl)(methyl)amino]-2-oxoethyl}carbamate in EtOAc was added 4 M HCl/EtOAc (10.0 mL, 40.0 mmol). After being stirred at room temperature for 2 h, the mixture was concentrated in vacuo and the residue was diluted with EtOH/EtOAc. The resulting precipitate was filtered to give the product (177 mg, 66%) as a light pink solid. ^{1}H NMR (DMSO-d_6): this compound exists as a pair of rotamers at room temperature. δ 1.27 (6H, t, J = 7.2 Hz), 2.91 (minor rotamer, 3H, s), 2.97 (major rotamer, 3H, s), 2.99–3.14 (4H, m), 3.89–4.00 (2H, m), 4.32 (2H, d, J = 5.6 Hz),

4.63 (minor rotamer, 2H, s), 4.64 (major rotamer, 2H, s), 7.26–7.33 (1H, m), 7.47 (major rotamer, 1H, dd, J = 7.6, 7.6 Hz), 7.52 (minor rotamer, 1H, dd, J = 7.6, 7.6 Hz), 7.53 (minor rotamer, 1H, s), 7.58 (major rotamer, 1H, s), 7.62 (major rotamer, 1H, d, J = 7.6 Hz), 7.67 (minor rotamer, 1H, d, J = 7.6 Hz), 7.71–7.80 (4H, m), 8.11–8.29 (3H, m), 10.92 (1H, br s); MS (FAB) m/z $[M+H]^+$ 340. Anal. Calcd for $C_{21}H_{29}N_3O{\cdot}2.1HCl{\cdot}1.8H_2O$: C, 56.24; H, 7.80; N, 9.37; Cl, 16.60. Found: C, 56.48; H, 7.95; N, 9.13; Cl, 16.87.

5.1.23. *N*-Methyl-1-[4′-(morpholin-4-yl)biphenyl-3-yl] methanamine (16)

To a mixture of *tert*-butyl (3-bromobenzyl)methylcarbamate (**14**; 2.10 g, 7.00 mmol) in DME (21 mL)/water(11 mL) were added 4-[4-(4,4,5,5-tetramethyl-1,3,2-dioxaborolan-2-yl)phenyl]morpholine (**15**; 2.12 g, 7.35 mmol), $Pd(PPh_3)_4$ (243 mg, 0.21 mmol) and Na_2CO_3 (2.22 g, 21.0 mmol). The mixture was stirred at 90 °C for 36 h. After being cooled to room temperature, the mixture was concentrated in vacuo. The residue was diluted with water and extracted with $CHCl_3$. The organic layer was dried over $MgSO_4$, and concentrated in vacuo. The residue was purified by column chromatography on silica gel ($CHCl_3$/MeOH = 98/2) to afford *tert*-butyl methyl{[4′-(morpholin-4-yl)biphenyl-3-yl]methyl} carbamate (2.20 g, 82%) as a colorless oil. To a solution of *tert*-butyl methyl{[4′-(morpholin-4-yl)biphenyl-3-yl]methyl}carbamate (1.82 g, 4.76 mmol) in EtOH (20 mL) was added 4 M HCl/EtOAc (10.0 mL, 40.0 mmol). After being stirred at room temperature for 24 h, the mixture was concentrated in vacuo. The residue was diluted with saturated $NaHCO_3$ aqueous solution, and the mixture was extracted with $CHCl_3$. The organic layer was dried over Na_2SO_4 and concentrated in vacuo to afford the product (1.24 g, 92%). ^{1}H NMR ($CDCl_3$): δ 2.49 (3H, s), 3.17–3.25 (4H, m), 3.81 (2H, s), 3.86–3.91 (4H, m), 6.95–7.01 (2H, m), 7.25 (1H, d, J = 7.7 Hz), 7.37 (1H, dd, J = 7.6, 7.6 Hz), 7.44–7.48 (1H, m), 7.51–7.57 (3H, m); MS (ESI) m/z $[M+H]^+$ 283.

5.1.24. *N*,*N*^{2}-Dimethyl-*N*-{[4′-(morpholin-4-yl)biphenyl-3-yl] methyl}glycinamide (2*R*,3*R*)-tartrate (17)

Compound **17** was prepared from **16** and *N*-(*tert*-butoxycarbonyl)-*N*-methylglycine in 43% yield, using a similar approach to that described for **11c**. ^{1}H NMR (DMSO-d_6): this compound exists as a pair of rotamers at room temperature. δ 2.57 (minor rotamer, 3H, s), 2.59 (major rotamer, 3H, s), 2.88 (minor rotamer, 3H, s), 2.93 (major rotamer, 3H, s), 3.10–3.21 (4H, m), 3.72–3.80 (4H, m), 4.11 (minor rotamer, 2H, s), 4.13 (major rotamer, 2H, s), 4.13 (2H, s, tartaric acid), 4.56 (minor rotamer, 2H, s), 4.61 (major rotamer, 2H, s), 7.00–7.07 (2H, m), 7.14–7.20 (1H, m), 7.37–7.59 (5H, m); MS (ESI) m/z $[M+H]^+$ 354; HRMS (ESI) m/z Calcd for $C_{21}H_{28}N_3O_2$ $[M+H]^+$: 354.2176. Found: 354.2175.

5.1.25. *N*,*N*^{2},*N*^{2}-Trimethyl-*N*-{[4′-(morpholin-4-yl)biphenyl-3-yl]methyl}glycinamide (2*R*,3*R*)-tartrate (18)

To a solution of **16** (200 mg, 0.71 mmol) in DCE (3.0 mL) were added *N*,*N*-dimethylglycine (80 mg, 0.78 mmol), WSCD·HCl (163 mg, 0.85 mmol), and HOBt (115 mg, 0.85 mmol). After being stirred at room temperature for 2 h, the mixture was diluted with saturated $NaHCO_3$ aqueous solution and extracted with $CHCl_3$. The organic layer was dried over Na_2SO_4, and concentrated in vacuo. The residue was purified by column chromatography on silica gel ($CHCl_3$/MeOH) to afford *N*,*N*^{2},*N*^{2}-trimethyl-*N*-{[4′-(morpholin-4-yl)biphenyl-3-yl]methyl}glycinamide. To a solution of *N*,*N*^{2},*N*^{2}-trimethyl-*N*-{[4′-(morpholin-4-yl)biphenyl-3-yl]methyl}glycinamide in EtOH (3.0 mL) was added (2*R*,3*R*)-tartaric acid (106 mg, 0.71 mmol). After being stirred at room temperature for 2 h, the mixture was concentrated in vacuo to give the product (261 mg, 71%) as a solid: ^{1}H NMR (DMSO-d_6): this compound exists as a pair of rotamers at room temperature. δ 2.43 (minor rotamer, 6H, s), 2.50 (major rotamer, 6H, s), 2.81 (minor rotamer, 3H, s), 2.96 (major rotamer, 3H, s), 3.13–3.19 (4H, m), 3.58 (minor rotamer, 2H, s), 3.69 (major rotamer, 2H, s), 3.73–3.78 (4H, m), 4.11 (2H, s, tartaric acid), 4.58 (major rotamer, 2H, s), 4.65 (minor rotamer, 2H, s), 7.00–7.06 (2H, m), 7.11–7.17 (1H, m), 7.35–7.47 (2H, m), 7.48–7.57 (3H, m); MS (ESI) m/z $[M+H]^+$ 368; Anal. Calcd for $C_{22}H_{29}N_3O_2{\cdot}C_4H_6O_6{\cdot}2H_2O$: C, 56.41; H, 7.10; N, 7.59. Found: C, 56.65; H, 6.92; N, 7.25.

5.1.26. *N*-Methyl-*N*-{[4′-(morpholin-4-yl)biphenyl-3-yl] methyl}-β-alaninamide (2*R*,3*R*)-tartrate (19)

Compound **19** was prepared from **16** and *N*-(*tert*-butoxycarbonyl)-β-alanine in 69% yield as a solid, using a similar approach to that described for **11c**. ^{1}H NMR (DMSO-d_6): this compound exists as a pair of rotamers at room temperature. δ 2.76 (2H, t, J = 6.4 Hz), 2.89 (minor rotamer, 3H, s), 2.94 (major rotamer, 3H, s), 2.99–3.24 (2H, m), 3.10–3.20 (4H, m), 3.70–3.79 (4H, m), 3.83 (2H, s, tartaric acid), 4.59 (major rotamer, 2H, s), 4.62 (minor rotamer, 2H, s), 6.97–7.07 (2H, m), 7.10–7.21 (1H, m), 7.34–7.59 (5H, m); MS (ESI) m/z $[M+H]^+$ 354; Anal. Calcd for $C_{21}H_{27}N_3O_2{\cdot}C_4H_6O_6{\cdot}0.7H_2O$: C, 58.17; H, 6.72; N, 8.14. Found: C, 58.02; H, 6.60; N, 8.20.

5.1.27. *N*,2-Dimethyl-*N*-{[4′-(morpholin-4-yl)biphenyl-3-yl] methyl}alaninamide (2*R*,3*R*)-tartrate (27)

To a mixture of **6** (500 mg, 2.50 mmol) in CH_2Cl_2 (5.0 mL) were added *N*-(*tert*-butoxycarbonyl)-2-methylalanine (533 mg, 2.62 mmol), WSCD·HCl (527 mg, 2.75 mmol), and HOBt (371 mg, 2.75 mmol). After being stirred at room temperature for 3 h, the mixture was diluted with water and extracted with $CHCl_3$. The organic layer was washed with HCl aqueous solution and saturated $NaHCO_3$ aqueous solution, dried over $MgSO_4$, and concentrated in vacuo. The residue was purified by column chromatography on silica gel ($CHCl_3$/MeOH = 98:2) to afford *tert*-butyl {1-[(3-bromobenzyl)(methyl)amino]-2-methyl-1-oxopropan-2-yl}carbamate (**23**) (915 mg, 95%) as a colorless oil. To a mixture of **23** (286 mg, 0.74 mmol) in DME (2.9 mL)/water (1.4 mL) were added **15** (225 mg, 0.78 mmol), Na_2CO_3 (236 mg, 2.23 mmol), and $Pd(PPh_3)_4$ (26 mg, 0.022 mmol). The mixture was stirred at 90 °C for 36 h. After being cooled to room temperature, the mixture was concentrated in vacuo. The residue was diluted with water and extracted with $CHCl_3$. The organic layer was dried over $MgSO_4$ and concentrated in vacuo. The residue was purified by column chromatography on silica gel ($CHCl_3$/MeOH = 98:2) to afford *tert*-butyl [2-methyl-1-(methyl{[4′-(morpholin-4-yl)biphenyl-3-yl] methyl}amino)-1-oxopropan-2-yl]carbamate (290 mg, 84%) as a colorless oil. To a solution of *tert*-butyl [2-methyl-1-(methyl{[4′-(morpholin-4-yl)biphenyl-3-yl]methyl}amino)-1-oxopropan-2-yl]-carbamate (290 mg, 0.62 mmol) in MeOH was added 4 M HCl/EtOAc. After being stirred at room temperature for 4 h, the mixture was concentrated in vacuo. The residue was diluted with saturated $NaHCO_3$ aqueous solution, and the mixture was extracted with $CHCl_3$. The organic layer was dried over Na_2SO_4 and concentrated in vacuo. To a solution of the residue in EtOH was added (2*R*,3*R*)-tartaric acid (93 mg, 0.62 mmol). The resulting precipitate was filtered to give the product (160 mg, 50%) as a colorless solid. ^{1}H NMR (DMSO-d_6): this compound exists as a pair of rotamers at room temperature. δ 1.55 (minor rotamer, 6H, s), 1.58 (major rotamer, 6H, s), 2.95–3.21 (7H, m), 3.73–3.78 (4H, m), 3.86 (2H, s, tartaric acid), 4.68 (2H, br s), 6.98 (minor rotamer, 2H, d, J = 8.9 Hz), 7.03 (major rotamer, 2H, d, J = 8.9 Hz), 7.12 (major rotamer, 1H, d, J = 7.5 Hz), 7.22 (minor rotamer, 1H, d, J = 7.5 Hz), 7.31–7.44 (2H, m), 7.46–7.57 (3H, m); MS (ESI) m/z $[M+H]^+$ 368; Anal. Calcd

for $C_{22}H_{29}N_3O_2{\cdot}C_4H_6O_6{\cdot}H_2O$: C, 58.31; H, 6.96; N, 7.85. Found: C, 58.57; H, 6.78; N, 7.83.

5.1.28. *N*-Isopropyl-*N*-{[4′-(morpholin-4-yl)biphenyl-3-yl] methyl}glycinamide (2*R*,3*R*)-tartrate (28)

Compound **28** was prepared from *N*-(3-bromobenzyl)propan-2-amine (**20**) and [(*tert*-butoxycarbonyl)amino]acetic acid in 72% yield, using a similar approach to that described for **27**. ^{1}H NMR (DMSO-d_6): this compound exists as a pair of rotamers at room temperature. δ 1.05–1.18 (6H, m), 3.08–3.22 (4H, m), 3.66 (minor rotamer, 2H, s), 3.71–3.79 (4H, m), 3.85 (2H, s, tartaric acid), 4.03 (major rotamer, 2H, s), 4.48–4.63 (3H, m), 6.97–7.08 (2H, m), 7.11–7.20 (1H, m), 7.29–7.58 (5H, m); MS (ESI) *m*/*z* $[M+H]^+$ 368; Anal. Calcd for $C_{22}H_{29}N_3O_2{\cdot}C_4H_6O_6{\cdot}0.6H_2O$: C, 59.10; H, 6.91; N, 7.95. Found: C, 58.97; H, 6.76; N, 7.95.

5.1.29. *N*-Methyl-*N*-{[4′-(morpholin-4-yl)biphenyl-3-yl]methyl} ethane-1,2-diamine (2*R*,3*R*)-tartrate (29)

To a solution of 1-bromo-3-(bromomethyl)benzene (**21**; 570 mg, 2.28 mmol) in DMF (6.0 mL) were added *tert*-butyl [2-(methylamino)ethyl]carbamate (400 mg, 2.30 mmol) and K_2CO_3 (630 mg, 4.56 mmol). After being stirred at room temperature overnight, the mixture was concentrated in vacuo. The residue was diluted with saturated $NaHCO_3$ aqueous solution and extracted with $CHCl_3$. The organic layer was dried over Na_2SO_4, and concentrated in vacuo. The residue was purified by column chromatography on silica gel ($CHCl_3$/MeOH) to afford *tert*-butyl {2-[(3-bromobenzyl)(methyl)amino]ethyl}carbamate (**25**; 782 mg, quantitative yield). To a mixture of **25** (500 mg, 1.46 mmol) in DME (5.0 mL)/water (2.0 mL) were added **15** (500 mg, 1.73 mmol), Na_2CO_3 (463 mg, 4.37 mmol), and Pd $(PPh_3)_4$ (55 mg, 0.048 mmol). The mixture was stirred at 80 °C overnight. After being cooled to room temperature, the mixture was concentrated in vacuo. The residue was diluted with saturated $NaHCO_3$ aqueous solution and extracted with $CHCl_3$. The organic layer was dried over Na_2SO_4 and concentrated in vacuo. The residue was purified by column chromatography on silica gel ($CHCl_3$/MeOH) to afford *tert*-butyl [2-(methyl{[4′-(morpholin-4-yl)biphenyl-3-yl]methyl}amino)ethyl]carbamate. To a solution of *tert*-butyl [2-(methyl{[4′-(morpholin-4-yl)biphenyl-3-yl]methyl}amino) ethyl]carbamate in EtOH (6.0 mL) was added 4 M HCl/EtOAc (3.00 mL, 12.0 mmol). After being stirred at room temperature overnight, the mixture was concentrated in vacuo. The residue was diluted with saturated $NaHCO_3$ aqueous solution, and the mixture was extracted with $CHCl_3$. The organic layer was dried over Na_2SO_4 and concentrated in vacuo. To a solution of the residue in EtOH was added (2*R*,3*R*)-tartaric acid (104 mg, 0.69 mmol). After being stirred at room temperature for 2 h, the mixture was concentrated in vacuo. To the residue was added EtOAc and the resulting precipitate was filtered to give the product (111 mg, 16%). ^{1}H NMR (DMSO-d_6): δ 2.16 (3H, s), 2.58 (2H, t, *J* = 6.2 Hz), 2.95 (2H, t, *J* = 6.2 Hz), 3.08–3.22 (4H, m), 3.58 (2H, s), 3.73–3.78 (4H, m), 4.02 (2H, s, tartaric acid), 7.03 (2H, d, *J* = 8.8 Hz), 7.26 (1H, d, *J* = 7.6 Hz), 7.37 (1H, dd, *J* = 7.6, 7.6 Hz), 7.50 (1H, d, *J* = 7.8 Hz), 7.52–7.65 (3H, m); MS (ESI) *m*/*z* $[M+H]^+$ 326; HRMS (ESI) *m*/*z* Calcd for $C_{20}H_{28}N_3O$ $[M+H]^+$: 326.2227. Found:326.2230.

5.1.30. *tert*-Butyl [2-(5-bromo-1,3-dihydro-2H-isoindol-2-yl)-2-oxoethyl]carbamate (26)

Compound **26** was prepared from 5-bromoisoindoline hydrochloride (**22**) and [(*tert*-butoxycarbonyl)amino]acetic acid in 48% yield, using a similar approach to that described for **7**. ^{1}H NMR ($CDCl_3$): δ 1.47 (9H, s), 4.00 (2H, d, *J* = 4.3 Hz), 4.74 (2H, d, *J* = 14.5 Hz), 4.79 (2H, d, *J* = 16.4 Hz), 5.48 (1H, br s), 7.17 (1H, dd, *J* = 8.1, 13.5 Hz), 7.42–7.48 (2H, m); MS (ESI) *m*/*z* $[M+H]^+$ 357.

5.1.31. 2-Amino-1-{5-[4-(morpholin-4-yl)phenyl]-1,3-dihydro-2H-isoindol-2-yl}ethanone hydrochloride (30)

Compound **30** was prepared from **26** and **15** in 85% yield as a solid, using a similar approach to that described for **4a**·**HCl**. ^{1}H NMR (DMSO-d_6): δ 3.21–3.35 (4H, m), 3.78–3.98 (6H, m), 4.75 (2H, d, *J* = 8.6 Hz), 4.91 (2H, d, *J* = 8.1 Hz), 7.25–7.33 (2H, m), 7.43 (1H, dd, *J* = 8.1, 10.8 Hz), 7.57–7.69 (4H, m), 8.36 (3H, br s); MS (ESI) *m*/*z* $[M+H]^+$ 338; HRMS (ESI) *m*/*z* Calcd for $C_{20}H_{24}N_3O_2$ $[M+H]^+$: 338.1863. Found:338.1865.

5.1.32. Methyl 4′-(morpholin-4-yl)biphenyl-3-carboxylate (32)

To a solution of methyl 3-bromobenzoate (**31**; 500 mg, 2.33 mmol) in DME (5.0 mL)/water (2.0 mL) were added **15** (700 mg, 2.42 mmol), Na_2CO_3 (739 mg, 6.98 mmol), and $Pd(PPh_3)_4$ (80 mg, 0.069 mmol). The mixture was stirred at 80 °C overnight. After being cooled to room temperature, the mixture was concentrated in vacuo. The residue was diluted with saturated $NaHCO_3$ aqueous solution and extracted with $CHCl_3$. The organic layer was dried over Na_2SO_4 and concentrated in vacuo. The residue was purified by column chromatography on silica gel ($CHCl_3$/MeOH) to afford methyl 4′-(morpholin-4-yl)biphenyl-3-carboxylate (531 mg, 77%). To a solution of methyl 4′-(morpholin-4-yl)biphenyl-3-carboxylate (531 mg, 1.79 mmol) in EtOH (10 mL) was added 1 M NaOH aqueous solution (5.00 mL, 5.00 mmol). The mixture was stirred at 60 °C for 3 h. After being cooled to room temperature, the mixture was neutralized with 1 M HCl aqueous solution. The resulting precipitate was filtered to give the product (470 mg, 93%) as a solid. ^{1}H NMR (DMSO-d_6): δ 3.12–3.21 (4H, m), 3.72–3.80 (4H, m), 7.05 (2H, d, *J* = 7.8 Hz), 7.52–7.63 (3H, m), 7.83–7.89 (2H, m), 8.11–8.15 (1H, m), 13.01 (1H, br s); MS (ESI) *m*/*z* $[M+H]^+$ 284.

5.1.33. *N*-(2-Aminoethyl)-*N*-methyl-4′-(morpholin-4-yl) biphenyl-3-carboxamide (2*R*,3*R*)-tartrate (33)

Compound **33** was prepared from **32** and *tert*-butyl [2-(methylamino)ethyl]carbamate in 34% yield, using a similar approach to that described for **11c**. ^{1}H NMR (DMSO-d_6): this compound exists as a pair of rotamers at room temperature. δ 2.96 (3H, br s), 3.03–3.21 (6H, m), 3.63–3.79 (6H, m), 3.87 (2H, s, tartaric acid), 6.97–7.09 (2H, m), 7.22–7.41 (1H, m), 7.43–7.54 (1H, m), 7.59 (major rotamer, 2H, d, *J* = 8.8 Hz), 7.64 (minor rotamer, 2H, d, *J* = 8.8 Hz), 7.69 (major rotamer, 2H, d, *J* = 7.3 Hz), 7.78 (minor rotamer, 2H, d, *J* = 7.4 Hz); MS (ESI) *m*/*z* $[M+H]^+$ 340; Anal. Calcd for $C_{20}H_{25}N_3O_2{\cdot}C_4H_6O_6{\cdot}0.6H_2O$: C, 57.61; H, 6.49; N, 8.40. Found: C, 57.61; H, 6.42; N, 8.37.

5.2. Molecular modeling

5.2.1. Human VAP-1 model

A side-chain conformational search and minimization for Leu469 of the three-dimensional (3D) structure of VAP-1 with TPQ in an active conformation (PDB-code: 2C11,[18] resolution: 2.90 Å) was performed using the Low Mode MD[19] function in the Molecular Operating Environment (MOE) program[16a] with an MMFF94x forcefield. The bound 2-hidrazinopyridine ligand was then deleted.

5.2.2. Docking study

The ligand molecules were prepared using LigPrep[20] and Confgen,[21] and the energy-minimized conformation was used to input molecules into the follow docking calculations. Compounds were docked to the human VAP-1 model using the docking program GOLD version 5.2.[22] The ligand-binding pocket was defined using $C^{\beta}H$ from Leu468 as the central atom with a radius of 20 Å. The ligand was docked covalently to nitrogen atom N1 of PAQ1729 (PAQ is used PDB entry 2C11[18]) to assign TPQ and the ligand. Each ligand was docked 10 times.

5.3. Inhibitory effect on human and rat VAP-1 enzyme activity

Human and rat VAP-1 enzyme activity was measured by a radiochemistry-enzymatic assay using ^{14}C-benzylamine (American Radiolabeled Chemicals, STL, USA).[23] An enzyme suspension prepared from CHO (Chinese Hamster Ovary) cells expressing a human or rat VAP-1 enzyme was preincubated with the test compound in a 96-well microplate at room temperature for 20 min. Subsequently, the enzyme suspension was incubated with ^{14}C-benzylamine (final concentration of 1×10^{-6} mol/L) to a final volume of 50 μL at 37 °C for 1 h. The enzymatic reaction was stopped by the addition of 2 mol/L (50 μL) of citric acid. The oxidation products were extracted directly in a 200-μL toluene scintillator, and the radioactivity was measured with a scintillation spectrometer.

5.4. Animal experiments

All animal experimental procedures were approved by the Institutional Animal Care and Use Committee of Astellas Pharma Inc. Further, Astellas Pharma Inc. Tsukuba Research Center was awarded Accreditation Status by the AAALAC International. All efforts were made to minimize the number of animals used and to avoid suffering and distress.

5.4.1. Inhibitory effect on plasma VAP-1 enzyme activities in rat

Male Wistar rats were purchased from Japan Charles River Laboratories (Yokohama, Japan). Blood samples for the measurement of VAP-1 activity were collected via the tail vein under diethyl ether anesthesia through a heparinized capillary. Blood was sampled before and 1 h after the orally dosing of test compounds. The collected blood was placed into sampling tubes (1.5 mL), cooled in iced water and centrifuged at 4 °C to obtain plasma. The resulting plasma was stored at −80 °C until measurement of plasma VAP-1 activity.

Plasma VAP-1 activity was measured using a radioenzyme assay with a substrate of ^{14}C-benzylamine (American Radiolabeled Chemicals, STL, USA)..[23] Total VAP-1 activity was measured by reacting a mixture of 80 or 100 μL rat plasma and 10 μL ^{14}C-benzylamine at 37 °C for 2 h, and non-specific activity was measured with 10 μL aminoguanidine hydrochloride (Sigma, STL, USA, 1 mmol/L), FR271207 or FR299676 (a specific VAP-1 inhibitor; Astellas Pharma Inc., 1 mmol/L) under the same conditions. Radioactivity of the reaction metabolite (^{14}C-benzaldehyde) was measured with a liquid scintillation counter (TRI-CARB 2100TR or TRI-CARB 3110TR; Perkin Elmer Japan, Yokohama, Japan). Total and non-specific VAP-1 activities (pmol) were calculated using the measured radioactivity and the radioactivity of a standard with ^{14}C-benzylamine. Plasma VAP-1 activity and inhibition ratio were calculated by the following formula:

$$\begin{aligned}&\text{Plasma VAP-1 activity (pmol/mL/h)}\\&= [\text{total activity (pmol)} - \text{non-specific activity (pmol)}]\\&\quad \times [1000/80 \text{ or } 100\ (\mu\text{L})]/2\ (\text{h}).\end{aligned}$$

$$\begin{aligned}&\text{Inhibition ratio (\%)}\\&= [\text{Plasma VAP-1 activity (before dosing)}\\&\quad - \text{Plasma VAP-1activity (1 h after dosing)}]\\&\quad /\text{Plasma VAP-1 activity (before dosing)}\end{aligned}$$

5.4.2. Stability in rat blood

Male Wistar rats were purchased from Charles River Laboratories Japan, Inc. (Yokohama, Japan). Blood was collected from the abdominal artery using heparin as an anticoagulant. Test compound solution of **3** or **4a** (hydrochloride salt) was added to the blood to prepare blood samples of 1 μg/mL, and then the blood sample was incubated at 37 °C for up to 6 h ($n = 3$). After incubation, test compound in the blood samples was extracted by deproteination with acetonitrile, and then analyzed by LC-MS/MS.

5.4.3. Rat pharmacokinetic study

Male Wistar rats were purchased from Charles River Laboratories Japan, Inc. (Yokohama, Japan). Rats were fasted for approximately 17 h before dosing. Compound **2** or **4g** was administered to rats ($n = 3$) either intravenously (iv) or orally (po) at a dose of 1 mg/kg. For the iv study, test compound was prepared as a solution of 10% DMF, 10% propylene glycol and 80% saline. For the po study, test compound was prepared as a solution of 10% DMF, 10% propylene glycol and 80% water. Blood was collected from the vein using heparin as an anticoagulant, immediately chilled on ice, and centrifuged to obtain plasma fraction. Test compound in plasma samples were extracted by deproteination with acetonitrile, and then analyzed by LC-MS/MS. Pharmacokinetic parameters were calculated from plasma concentrations of test compound using the non-compartmental analysis model.

5.5. Permeability study using artificial membrane

Parallel artificial membrane permeability assays (PAMPA) conducted in this study used the PAMPA Evolution from *p*ION Inc. (Billerica, MA). In this assay, a 'sandwich' is formed from a 96-well microtiter plate (*p*ION Inc.) and a 96-well filter plate (*p*ION Inc.), so that each composite well is divided into two chambers, with a donor at the bottom and an acceptor at the top, separated by a microfilter disc coated with lipid (*p*ION Inc.) in each well. Drug samples were introduced as a 10 mM dimethyl sulfoxide (DMSO) stock solution in a 96-well polypropylene microtiter plate. The robotic liquid handling system draws a 5 μL aliquot of the DMSO stock solution and mixes it into an aqueous buffer solution of 10% (v/v) DMSO to attain a final typical sample concentration of 50 μM. The drug solutions were filtered using a 96-well filter plate (polyvinylidene fluoride; Corning Inc., Corning, NY) and added to the donor compartments. The donor solution was adjusted to pH 6.5 (NaOH-treated buffer; *p*ION Inc.), whereas the acceptor solution had a pH of 7.4 (*p*ION Inc.). The plates were sandwiched together and incubated at room temperature for 2 h in a humidity-saturated atmosphere. After incubation, the sandwiched plates were separated, and both the donor and acceptor compartments were assayed for the amount of material present by comparison of the peak heights by HPLC. Mass balance, which is the difference between the reference and the sum of the donor and acceptor, was used to determine the amount of material remaining in the membrane barrier. The permeability (P_e) was calculated using PAMPA Evolution software (*p*ION Inc.).

5.6. Plasma protein binding study

Plasma was obtained from male Wistar rats purchased from Charles River Laboratories Japan, Inc. (Yokohama, Japan). Test compound solution of **4a** (hydrochloride salt), **4b** or **4g** was added to the plasma to prepare plasma samples of 2 μM. The plasma sample and PBS were transferred into the sample chamber and buffer chamber of a RED device (Thermo Fisher Scientific Inc., USA), respectively ($n = 3$). The dialysis device was placed on an orbital shaker in a CO_2 incubator set at 37 °C and 5% CO_2, and incubated for 16 h. After incubation, the plasma sample and PBS sample were collected from the two chambers, and mixed with the same volume of blank PBS and blank plasma, respectively. Test compound in mixed samples was extracted by deproteination with acetonitrile, and then analyzed by LC-MS/MS.

The plasma protein binding ratio (%) and plasma unbound fraction (f_p) were calculated using the following equations:

$$\text{Plasma protein binding ratio } (\%) = (1 - f_p) \times 100$$

$$f_p = C_f / C_p$$

where 'C_f' is the concentration of test compound in a PBS sample after dialysis, and 'C_p' is the concentration of test compound in a plasma sample after dialysis.

Acknowledgements

The authors thank the staff of the Astellas Research Technologies Co., Ltd. for conducting PAMPA assays, elemental analysis, and spectral measurements. The authors also thank Mr. Kyoichi Maeno and Dr. Susumu Watanuki for their valuable advice in the preparation of this manuscript and Dr. Toshio Okazaki for his support.

References and notes

1. Pannecoeck, R.; Serruys, D.; Benmeridja, L.; Delanghe, J. R.; van Geel, N.; Speeckaert, R.; Speeckaert, M. M. *Crit. Rev. Clin. Lab. Sci.* **2015**, *52*, 284.
2. (a) Merinen, M.; Irjala, H.; Salmi, M.; Jaakkola, I.; Hänninen, A.; Jalkanen, S. *Am. J. Pathol.* **2005**, *166*, 793; (b) Mazzone, T.; Chait, A.; Plutzky, J. *Lancet* **1800**, *2008*, 371.
3. Buffoni, F.; Ignesti, G. *Mol. Genet. MeTable* **2000**, *71*, 559.
4. (a) Boomsma, F.; van den Meiracker, A. H.; Winkel, S.; Aanstoot, H. J.; Batstra, M. R.; Man in 't Veld, A. J.; Bruining, G. J. *Diabetologia* **1999**, *42*, 233; (b) Abella, A.; García-Vicente, S.; Viguerie, N.; Ros-Baró, A.; Camps, M.; Palacín, M.; Zorzano, A.; Marti, L. *Diabetologia* **2004**, *47*, 429; (c) Boomsma, F.; Bhaggoe, U. M.; van der Houwen, A. M.; van den Meiracker, A. H. *Biochim. Biophys. Acta* **2003**, *1647*, 48.
5. (a) Yu, P. H.; Wright, S.; Fan, E. H.; Lun, Z. R.; Gubisne-Harberle, D. *Biochim. Biophys. Acta* **2003**, *1647*, 193; (b) Hernandez, M.; Solé, M.; Boada, M.; Unzeta, M. *Biochim. Biophys. Acta* **2006**, *1763*, 164.
6. (a) Marttila-Ichihara, F.; Smith, D. J.; Stolen, C.; Yegutkin, G. G.; Elima, K.; Mercier, N.; Kiviranta, R.; Pihlavisto, M.; Alaranta, S.; Pentikäinen, U.; Pentikäinen, O.; Fülöp, F.; Jalkanen, S.; Salmi, M. *Arthritis Rheum.* **2006**, *54*, 2852; (b) Akin, E.; Aversa, J.; Steere, A. C. *Infect. Immun.* **2001**, *69*, 1774.
7. Mészáros, Z.; Karádi, I.; Csányi, A.; Szombathy, T.; Romics, L.; Magyar, K. *Eur. J. Drug Metab. Pharmacokinet.* **1999**, *24*, 299.
8. Boomsma, F.; van Veldhuisen, D. J.; de Kam, P. J.; Man in't Veld, A. J.; Mosterd, A.; Lie, K. I.; Schalekamp, M. A. D. H. *Cardiovasc. Res.* **1997**, *33*, 387.
9. (a) Yu, P. H. *Med. Hypotheses* **2001**, *57*, 175; (b) del Mar Hernandez, M.; Esteban, M.; Szabo, P.; Boada, M.; Unzeta, M. *Neurosci. Lett.* **2005**, *384*, 183.
10. Dunkel, P.; Balogh, B.; Meleddu, R.; Maccioni, E.; Gyires, K.; Mátyus, P. *Expert Opin. Ther. Pat.* **2011**, *21*, 1453.
11. (a) Smith, D.; Vainio, P.; Mikkola, J.; Vuorio, P.; Vainio, J. WO 2008129124, 2008.; (b) VAP-1 antibody product profile, Biotie, 2015. Available from: http://www.biotie.com/product-portfolio/vap1-antibody.aspx?sc_lang=en (last accessed August 2016).
12. (a) Schilter, H. C.; Collison, A.; Russo, R. C.; Foot, J. S.; Yow, T. T.; Vieira, A. T.; Tavares, L. D.; Mattes, J.; Teixeira, M. M.; Jarolimek, W. *Respir. Res.* **2015**, *16*, 42; (b) Jarolimek, W.; Charlton, B. *J. Hepatol.* **2015**, *62*, S274.
13. (a) Inoue, T.; Morita, M.; Tojo, T.; Yoshihara, K.; Nagashima, A.; Moritomo, A.; Ohkubo, M.; Miyake, H. *Bioorg. Med. Chem.* **2013**, *21*, 1219; (b) Inoue, T.; Morita, M.; Tojo, T.; Nagashima, A.; Moritomo, A.; Imai, K.; Miyake, H. *Bioorg. Med. Chem.* **2013**, *21*, 2478; (c) Inoue, T.; Morita, M.; Tojo, T.; Nagashima, A.; Moritomo, A.; Miyake, H. *Bioorg. Med. Chem.* **2013**, *21*, 3873.
14. Testa, B.; Mayer, J. M. *Hydrolysis in Drug and Prodrug Metabolism: Chemistry, Biochemistry, and Enzymology*, 2006. Chapter 4, 81.
15. (a) Kansy, M.; Senner, F.; Gubernator, K. *J. Med. Chem.* **1998**, *41*, 1007; (b) Clark, D. E.; Grootenhuis, P. D. J. *Curr. Top. Med. Chem.* **2003**, *3*, 1193.
16. (a) Molecular Operating Environment (MOE), 2010.10; Chemical Computing Group Inc., 1010 Sherbrooke St. West, Suite #910, Montreal, QC, Canada, H3A 2R7, 2010.; (b) MOE2014.0901, Chemical Computing Group Inc., 1010 Sherbrooke St. West, Suite #910, Montreal, QC, Canada, H3A 2R7, 2014.
17. ACD/Percepta, version 14.0.0, Advanced Chemistry Development Inc, Toronto, ON, Canada, www.acdlabs.com, 2013.
18. Jakobsson, E.; Nilsson, J.; Ogg, D.; Kleywegt, G. J. *Acta Crystallogr., Sect. D: Biol. Crystallogr.* **2005**, *61*, 1550.
19. Labute, P. *J. Chem. Inf. Model.* **2010**, *50*, 792.
20. LigPrep, version 2.5; Schrödinger, LLC, New York, NY, 2012.
21. Confgen, version 2.3; Schrödinger, LLC, New York, NY, 2012.
22. (a) GOLD5.2, The Cambridge Crystallographic Data Centre, Cambridge, UK.; (b) Jones, G.; Willett, P.; Glen, R. C. *J. Comput. Aided Mol. Des.* **1995**, *9*, 532; (c) Jones, G.; Willett, P.; Glen, R. C.; Andrew, R. L.; Robin, T. *J. Mol. Biol.* **1997**, *267*, 727.
23. Hayes, B. E.; Clarke, D. E. *Res. Commun. Chem. Pathol. Pharmacol.* **1990**, *69*, 71.